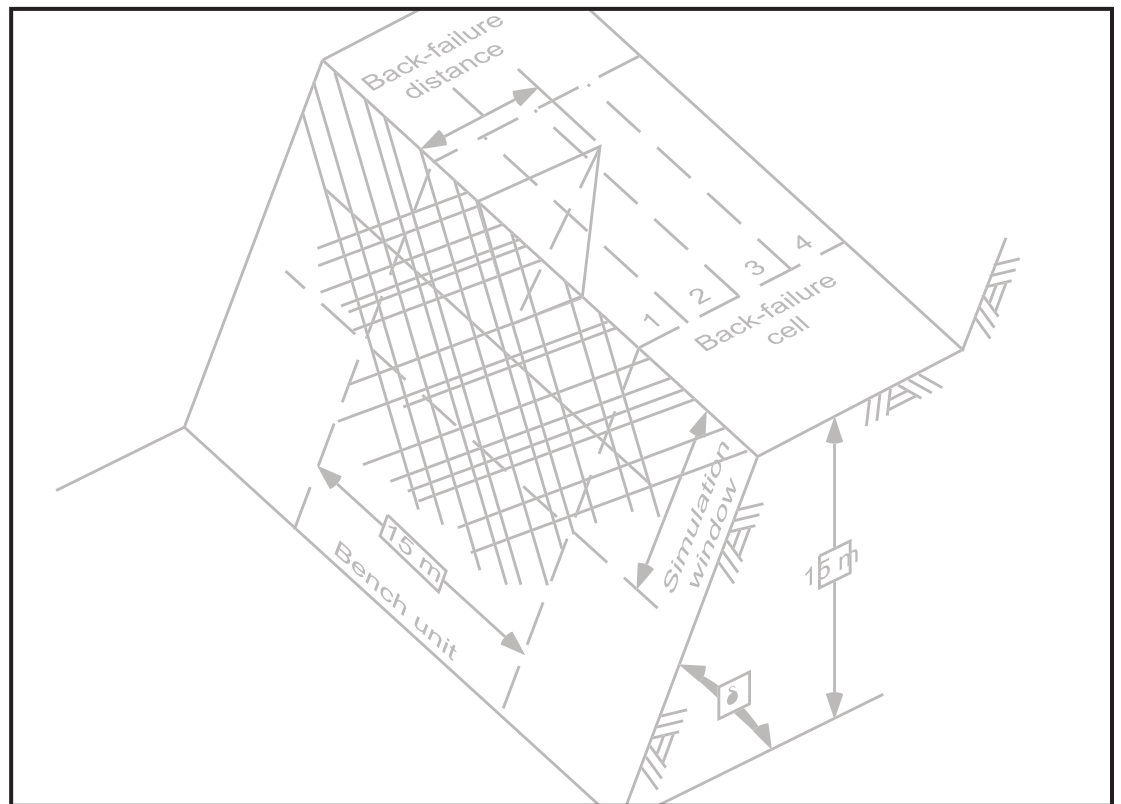CDC
Workplace
Safety and Health

# A User's Guide for the Bplane, Bstepp, and Bwedge Computer Programs

NIOSH

**INFORMATION CIRCULAR 9494**


# A USER'S GUIDE FOR THE BPLANE, BSTEPP, AND BWEDGE COMPUTER PROGRAMS

**By Stanley Miller, Jeffrey Whyatt, Jamie Girard Dwyer, and Edward McHugh**

## DISCLAIMER

Mention of any company or product does not constitute endorsement by the National Institute for Occupational Safety and Health (NIOSH). In addition, citations to Web sites external to NIOSH do not constitute NIOSH endorsement of the sponsoring organizations or their programs or products. Furthermore, NIOSH is not responsible for the content of these Web sites.

## ORDERING INFORMATION

To receive documents or other nformation about occupational safety and health topics, contact NIOSH at

NIOSH—Publications Dissemination
4676 Columbia Parkway
Cincinnati, OH  45226-1998

Telephone: **1-800-35-NIOSH**
Fax: 513-533-8573
e-mail: pubstaft@cdc.gov

or visit the NIOSH Web site at **www.cdc.gov/niosh**

**SAFER • HEALTHIER • PEOPLE™**

# TABLE OF CONTENTS

## FIGURES

## UNIT OF MEASURE ABBREVIATIONS USED IN THIS REPORT

| | | | |
|---|---|---|---|
| cm | centimeter | $t/m^3$ | tonnes per cubic meter |
| m | meter | ° | degree |
| $m^2$ | square meter | % | percent |
| min | minute | ft | foot |
| $t/m^2$ | tonnes per square meter | | |

# A USER'S GUIDE FOR THE BPLANE, BSTEPP, AND BWEDGE COMPUTER PROGRAMS

S. Miller,[1] J. Whyatt,[2] J. Girard Dwyer,[2] and E. McHugh[3]

## ABSTRACT

This user's guide covers the operation of a suite of three computer programs—Bplane, Bstepp, and Bwedge. These programs can be used to evaluate the potential for plane shear, step-path, and wedge failures along the crest of a slope bench. Such failures reduce the width of a catch bench and may compromise the bench's ability to catch rolling or sliding material before it reaches miners working below. The Bplane and Bwedge programs address sliding of blocks defined by continuous planar joints. The Bstepp program examines sliding of blocks defined by more complex failure surfaces that include steeply dipping cross joints and may even include breaks across small bridges of intact rock. The programs are applicable to jointed rock masses where the joints are small relative to the overall slope and form a number of sets with uniform statistical characteristics within a slope sector. The theoretical basis, application, and operation of these programs are described.

[1]Professor, University of Idaho, Moscow, ID.

[2]Mining engineer, Spokane Research Laboratory, National Institute for Occupational Safety and Health, Spokane, WA.

[3]Physical scientist, Spokane Research Laboratory, National Institute for Occupational Safety and Health, Spokane, WA.

# INTRODUCTION

This user's guide was developed by personnel at the National Institute for Occupational Safety and Health (NIOSH) as part of a program to protect miners who work on and beneath rock slopes. The guide covers operation of three related computer programs—Bplane, Bstepp, and Bwedge—that can be used to evaluate the potential for plane shear, step-path, and wedge failures along the crest of a slope. They are intended for use in the design of catch benches, but can be applied to analyses of failure along any crest in an appropriate rock mass. These programs are enhanced versions of codes originally developed by Miller [1982, 1984].

Catch benches are periodic flat breaks in a slope designed to catch raveling, sliding, and rolling slope material (figure 1). Bench crests are often allowed to fail locally, which creates an uneven crest (figure 2). Such failures are tolerable if the bench is maintained at sufficient width to provide protection for miners working below. Most failures occur as a result of initial excavation, during which failed material is removed. Other failures may occur later, after weathering, vibration, freeze-thaw cycles, etc., have generated debris that can load underlying benches or fall onto work areas if no additional measures are taken.
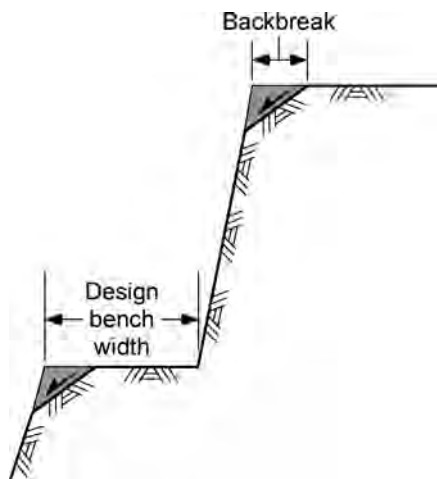


Figure 1. Typical catch-bench geometry (side view).
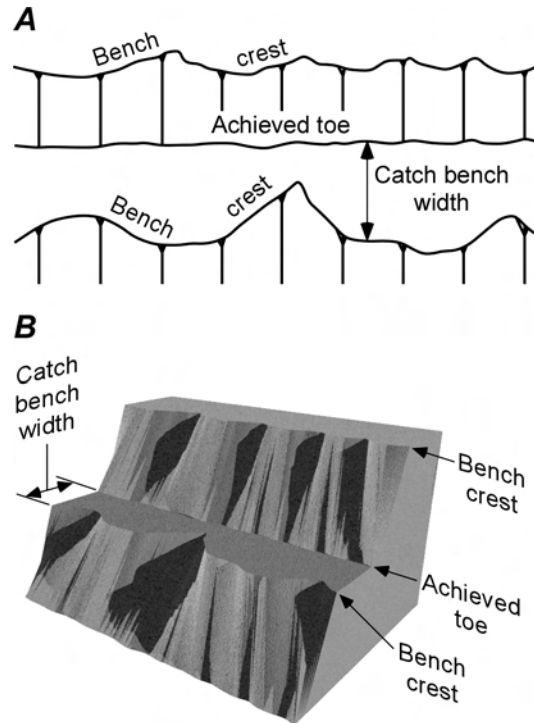


Figure 2. Plan view (A) and perspective (B) of realized bench width (after Ryan and Pryor, 2001).

Accident statistics collected by the Mine Safety and Health Administration (MSHA) have shown that bench failure and loose material moving down slopes pose significant safety hazards to miners. For instance, highwall failures and rock falls have contributed to 17 fatalities during a recent 5-year period (1996-2000). Of these, 12 occurred in metal/nonmetal mines and five in surface coal mines (figure 3). All five surface coal mine fatalities were attributed to "material falling from above," as were seven of the deaths in metal/nonmetal mines; two of these occurred while the victim was inside the cab of a piece of mining equipment. The remaining fatalities occurred when unstable or weakened highwalls collapsed beneath workers, most of whom were operating equipment on a bench or on top of a highwall.

The importance of bench integrity is well illustrated by two of these accidents. One oc-

curred on the evening of October 5, 1998, early in the night shift. A large piece of rock fell 6 m from the highwall to a safety bench, split, then fell an additional 16.6 m onto the cab of a drill, destroying the cab (figure 4). The rock measured about 2.3 m long, 2 m wide, and 1.2 m thick.

Another fatal accident occurred on the morning of September 2, 1998, when a 67-year-old bulldozer operator with 40 years of mining experience was maneuvering his Caterpillar D8 along a bench in a limestone quarry in Oregon. The outside edge of the bench collapsed, and the dozer rolled sideways 2-1/2 times to the bottom of the pit, coming to rest on its side. The dozer was equipped with rollover protection and a seat belt. The operator was not wearing the seat belt and was fatally injured.

This guide begins by examining the proper context in which the computer programs can be applied to assessments of bench safety. That is, when the programs can be used to provide insights into bench design and how results relate to results of other commonly used analysis methods. This discussion is followed by program operation and interpretation of output. Appendices provide



Figure 4. Cab crushed by slope failure (MSHA fatalgram, www.msha.gov).

definitions of key terms, a summary of data collection methods, and a review of the computational procedures. Appendix H provides a comprehensive list of input parameters, a useful reference on data input compilation.



Figure 3. Pie chart showing numbers of fatalities in coal and metal/nonmetal surface mines caused by failure of benches above and below workers for the period 1996-2000. Failure of benches above allows material to reach workers. Failure of benches below causes workers, especially those operating heavy equipment, to fall with failing bench material.

# BACKGROUND

A variety of engineering analyses can be conducted in support of rock slope design, depending on the purpose, service life, and geologic setting of the slope. The programs described in this package are applicable to only a small portion of these analyses, primarily those aimed at assessing retention of catch-bench width in highly jointed rock masses. Since fractures are too numerous to map and analyze individually in such a rock mass, a stochastic (probabilistic) approach is used. Thus, good results depend on accurate and representative statistical descriptions of fracture geometry and properties. They also depend on these statistical descriptions being valid throughout the area of interest.

Bench-scale failures in this type of rock mass most commonly occur in the upper portion of the bench where the fracture lengths required to define a potential failure block are shorter. The programs check for kinematically feasible plane shear, step-path, and wedge failures along the crest of a bench, and then compare the driving and resisting forces for each. The effect of failing blocks on bench width is then evaluated, and the probability of retaining various bench widths is reported. The surviving bench width, not the nominal planned width, should be used for evaluating whether a catch-bench design is adequate.

The capabilities of each program can be summarized as follows:

- The *Bplane* program analyzes plane shear failure modes in a two-dimensional framework by simulating plane shear fractures in the bench and then calculating the probability of stability for each one, as well as identifying the corresponding back-break distance on the bench. By repeating the simulation many times for a given bench, the probability of retaining various bench widths can be estimated.

- The *Bstepp* program conducts two-dimensional plane simulations for potential step-path failures comprised of a master joint set and a cross-joint set.

- The *Bwedge* program analyzes three-dimensional wedges by simulating fractures from two fracture sets and conducting a similar back-break analysis.

While these programs bring powerful stochastic tools to the analysis of some bench stability problems, they also have important limitations that must be recognized. First and foremost, the programs make specific assumptions about the geometry of failing blocks. More complex sets of discontinuities, failures of intact slope material, and wedge failures involving step-paths are not considered. Nor do these programs directly address the possibility that additional weakening through creep, weathering of rock materials, surface water runoff, freeze-thaw cycles, earthquake and blast vibrations, operation of equipment on haul roads, etc., can cause material to ravel or be released.

In addition, important failure modes, including rotational shear, block flow, toppling, and thin-slab (buckling) failure, are not considered. Rotational shear failures are typically found in soils and can be generated in slopes without critically oriented discontinuities or planes of weakness. Block flow failures are characterized by progressive breakdown of a rock slope. For instance, failure may be initiated in the toe of the slope, which in turn causes load transfer to adjacent areas that may fail, extending the failed zone.

Finally, the programs do not directly address filling of benches, nor whether a collapse might be caused by the weight of caught material and/or any equipment working on the bench.

# APPLICATION OF MODELS TO SLOPE DESIGN

Any analysis of slope stability necessarily starts with field investigations of the engineering geology of the rock mass (appendix B). Identification of which potential failure modes are possible and the scales at which they act are an important element of the investigation. Analysis of each failure mode is based on an idealized mathematical model, and a physical assumption is made (and, ideally, verified) that the slope is likely to act like the mathematical model. Such models define failure as inelastic movement of rock slope material from its original location in the planned slope geometry. This definition of failure does not necessarily imply an engineering failure of the slope system.

Whether or not failure in a safety sense (where does failing material go?) or an economic sense (what is the cost of the failure compared to the cost of a flattened or better-supported slope?) will occur requires additional analyses. For example, minor failure (raveling) of material in the slope face (perhaps as a result of weathering) might be tolerated if this failure occurs slowly with respect to pit life, and provisions can be made to control the consequences of such failure. That is, limited slope failure is tolerable so long as it does not pose a threat to miner safety or mine economic performance.

Common physical assumptions for slope failure modes have been validated through experience, some of which has been documented in case studies. The physical parameters required for each mathematical model are estimated and used to determine whether failure is likely under particular conditions. The accuracy and precision of this determination are sensitive to a number of factors, including validity of physical assumptions and the amount and type of geologic information available.

Mathematical models of the failure modes considered by these programs are described in the remainder of this section.

## PLANE SHEAR FAILURE

A plane shear failure occurs when a block defined by fractures and bench geometry slides along a single failure surface. The plane shear failure mode is said to be "kinematically viable" if the average strike is parallel or nearly parallel to the strike of the slope face and the dip is flatter than the dip of the slope face [Hoek and Bray 1981]. Failure will extend laterally along the bench to cross-cutting fractures, changes in bench orientation, and/or newly created fractures that provide release surfaces (figure 5). It is assumed that these surfaces will provide little resistance to sliding, so they can be neglected in assessing the stability of the block.

Hoek and Bray describe the geometrical conditions required for plane failure as follows:

A. The plane on which sliding occurs must strike approximately parallel or nearly parallel (within approximately ±20°) to the slope face.

B. The failure plane must "daylight" in the slope face. This means that its dip must be smaller than the dip of the slope face, that is, $\psi_f$ [slope face dip] $> \psi_p$ [fracture plane dip].

C. The dip of the failure plane must be greater than the angle of friction of this plane [in the absence of pore pressure], that is, $\psi_p$ [fracture plane dip] $> \varphi$ [fracture friction angle].

D. Release surfaces which provide negligible resistance to sliding must be present in the rock mass to define the lateral boundaries of the slide. Alternatively, failure can occur on a failure plane passing through the convex "nose" of a slope.
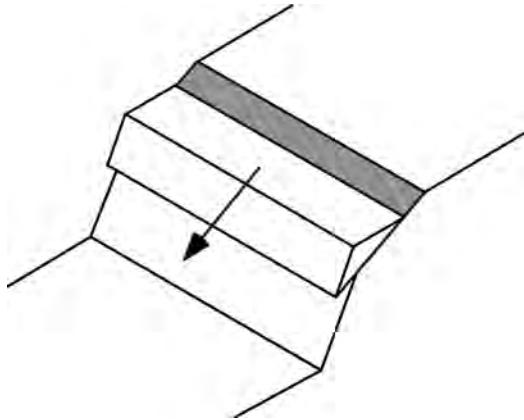
Figure 5. Idealized plane shear failure.

## STEP-PATH FAILURE

The availability of a single sliding surface that is long enough to permit plane shear failure may be comparatively rare if fractures are short. However, a more complex failure path comprised of multiple fractures is still possible, particularly where two conjugate fracture sets can form a stepped failure plane geometry [Jaeger 1971]. In this case, both sets strike parallel or nearly parallel to the strike of the slope, and the block slides on the flatter-dipping set (which usually dips at 20° to 50°). The steeper set creates release surfaces that connect to the sliding surfaces provided by the flatter set. The failure surface may also contain fractures which have broken small bridges of intact rock. Figure 6 illustrates a typical step-path geometry in a fractured rock slope.

Call and Nicholas [1978] describe criteria for generating potential step-path failure geometries starting from the point where a fracture in the master joint set intersects the bench face.

1. At least two fracture sets characterize a step-path geometry. The master set intersects the slope surface, and the cross set is steeper than the master set.

2. The fracture sets have strikes parallel or nearly parallel to slope strike.

3. Fracture set characteristics, including dip, length, and spacing, can be de-scribed by statistical distributions.

4. Under tensile stress, an existing fracture will propagate along its plane until it intersects another fracture, but not beyond.

5. A rock bridge is more likely to fail in tension than in shear.

6. Cross joints that do not intersect, but come within approximately 5 cm of the end of a master joint, are still considered part of the geometry that would allow the path to continue to the next master joint.

7. The flattest path is followed; that is, the step-path will follow a master joint to the cross joint farthest up the master joint. The path will then follow the cross joint until it intersects and continues along another master joint.

As the step-path geometry approaches a plane failure geometry, the step-path analysis may produce higher probabilities of failure. This is because a small rock bridge or jog in the failure surface accommodated by a cross-joint will not automatically prevent failure. However, the length of rock bridges that can be broken is
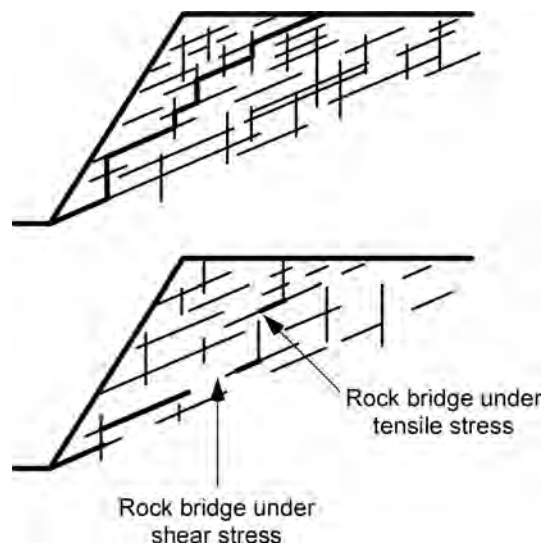


Figure 6. Examples of step-path geometries in rock slope (from Call and Nicholas, 1978). Top, continuous step-path; bottom, discontinuous step-path with intact rock bridges.

typically quite small. For instance, experience has shown that for benches 12 to 20 m high and cut in crystalline rock (tensile strength of 500 to 2,000 $t/m^2$), the probability of sliding is nearly zero when the fraction of intact rock along a step-path exceeds approximately 0.08. Thus, step-paths where bridges constitute 8% or less of total length are likely to be assigned a higher risk of failure in a step-path analysis than in a comparable plane shear analysis.

## WEDGE FAILURE

Wedge-shaped blocks are found in benches where two intersecting fractures daylight in both bench and slope (figure 7). Failing wedges are assumed to maintain contact with both bounding fracture surfaces as they slide down

the interaction line. Cases in which a wedge-shaped block slides on a single bounding fracture surface and loses contact with the other are not considered. In the absence of pore pressure, sliding will occur only when the inclination of the intersection line is steeper than the friction angle of the fractures. If multiple fracture sets with wedge-forming potential are present, separate analyses must be conducted on each possible pair.



Figure 7. Idealized wedge failure.

# GEOTECHNICAL PROGRAM INPUT

The quality of a slope stability analysis depends on proper understanding and quantification of the geologic environment. This understanding should include knowledge of what failure modes are possible and the geologic characteristics of the various structural domains (figure 8). Structural domains should be further subdivided into analysis sectors with common bench dimensions and orientations. While geologic characteristics will persist throughout a domain, the relevance of various features will

depend on the bench orientation and geometry defined for each sector. Input can be divided into three main classes: fracture-set geometry, fracture shear strength, and rock mass properties. Any planes of weakness within intact rock can be considered as fractures with non-zero cohesion.

## FRACTURE SETS

Large-scale geologic structures that are continuous over distances comparable to an entire
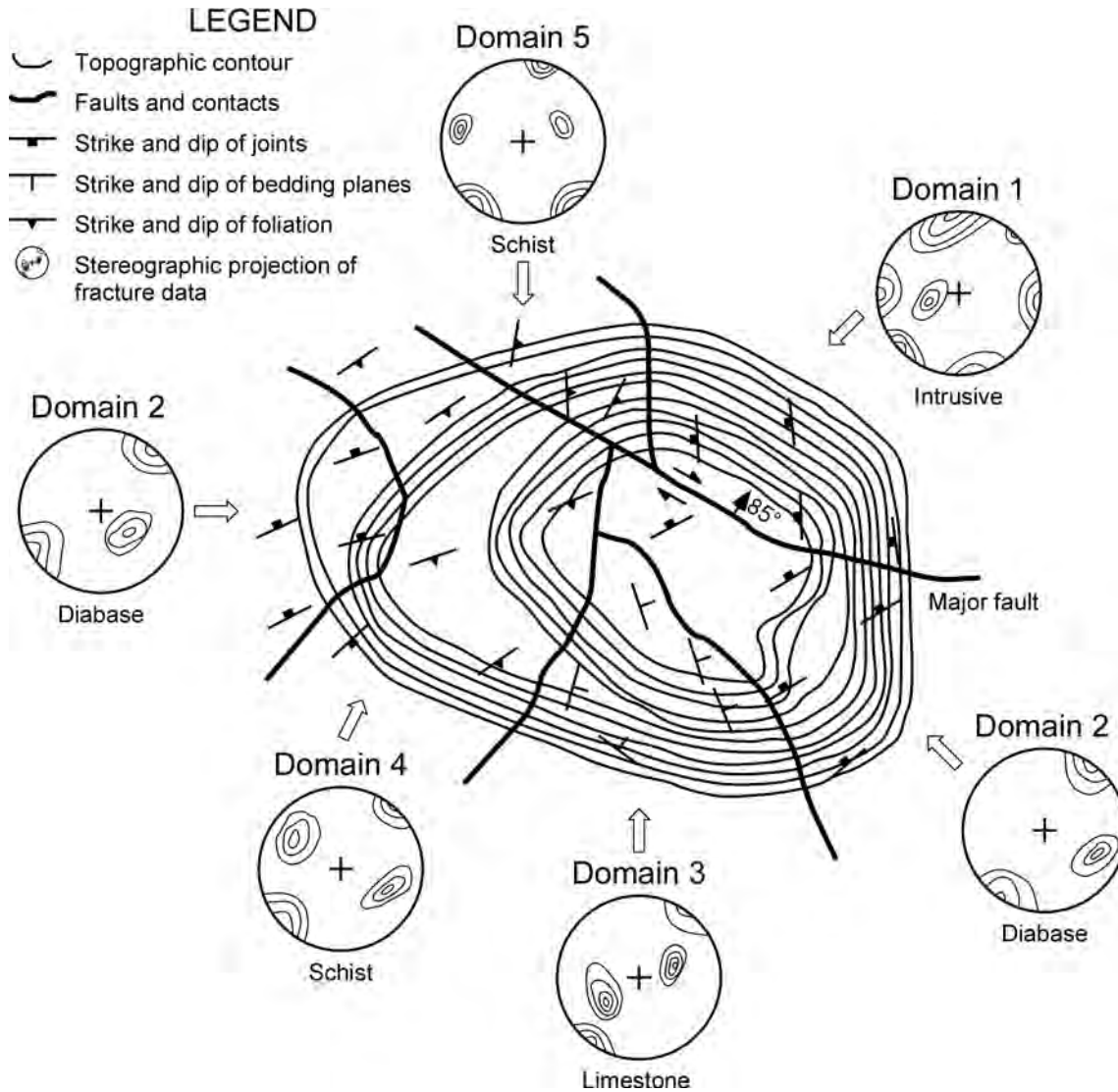
Figure 8. Example plot of structural domains in open-pit mine (after Nicholas and Sims, 2001).
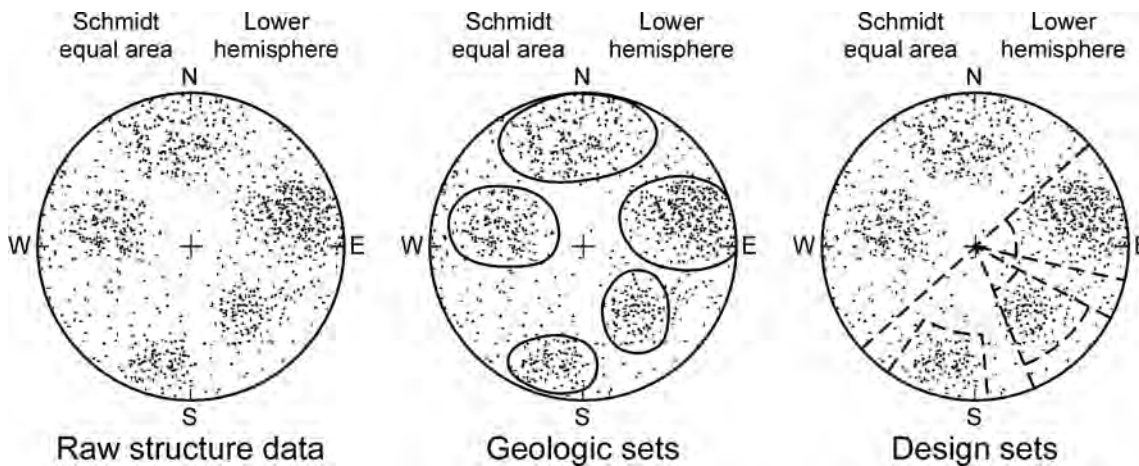


Figure 9. Example plot of structural domains in open-pit mine (after Nicholas and Sims, 2001).

slope or a project are generally mapped and addressed individually in the design process. Fractures (including joints and other planes of weakness) in rock slopes that compromise bench crest stability are generally too numerous to map individually and tend to be discontinuous. However, the natural processes that create these features tend to work systematically, generating patterns of fractures that can be understood in the aggregate. Thus, fractures can often be sorted into sets that contain fractures with similar orientations and with characteristics that can be described statistically.

Fracture mapping has three objectives: (1) identification of fracture sets, (2) definition of regions that contain distinctive fracture set patterns, and (3) definition of fracture set characteristics. Fracture set characteristics used by the programs described in this manual are fracture length (persistence), spacing, waviness, and orientation (dip and dip direction).

Fractures are sampled (mapped) at discrete locations throughout the region of interest. Three of the most common sampling methods are cell mapping [Call et al. 1976], set mapping [Call et al. 1976], and detail line mapping [Piteau, 1970; Call et al. 1976].

- *Cell mapping* is used where there are large, extensive exposures of rock, such as along benches in an open pit or in large natural outcrops. Consecutive mapping cells are established along the strike of the exposure, and information is recorded for each observed fracture set. Based on experience, Call and Savely [1990] recommend 30 to 40 cells for each structural domain described.

- *Set mapping* is used in place of cell mapping when rock exposures are not suitable for establishing consecutive cells or for reconnaissance-type mapping. This method provides information on fracture set orientations and characteristics, but not systematic informa-

tion from a large contiguous area.

- *Detail line mapping* has the least observer bias since all individual fractures are mapped along a line. It is most useful for initial studies prior to identification of fracture patterns. It is also the most tedious and provides the least amount of spatial coverage. The small amount of spatial coverage may bias the sampling (particularly for some line placements and orientations with respect to fracture set geometry).

Once field data are obtained, the first analytical step typically consists of plotting the poles to fractures on a lower-hemisphere stereonet in order to identify fracture sets, which appear as clusters of poles [Hoek and Bray 1981]. These plots are used to identify fracture sets, establish structural domains, and assess possible failure modes. Call and Savely [1990] recommend examining poles in conjunction with slope geometry and failure modes when identifying critical fracture sets (figure 9).

Each property of these fracture sets can be defined by a probability density function, or pdf. These programs use the normal pdf (fracture dip, dip direction), the exponential pdf (fracture spacing, length), and the right-skewed beta pdf (waviness). Spatial dependence in fracture properties can be described in geostatistical terms [La Pointe 1980; Miller 1979]. Semivariograms [Isaaks and Srivastava 1989] provide a statistical format for describing the spatial dependence of fracture property variability as a function of the lag count separation of fractures in a set. These statistical models are briefly defined in appendix A, and a more detailed treatment is provided in appendix C. A full list of input parameters is provided in appendix H.

## FRACTURE SET SHEAR STRENGTH

Shear strength along rock fractures is typically estimated in one of two ways. The joint

roughness coefficient-joint wall compressive strength (JRC-JCS) method proposed by Barton [1973] relies on a nonlinear failure envelope based on joint roughness coefficient (JRC), joint wall (that is, intact rock) compressive strength (JCS), and a base friction angle (that is, the friction angle associated with planar, saw-cut surfaces of the rock). The other shear-strength method (the one used for these bench stability programs) relies on laboratory direct-shear test data, or approximations thereof, to describe a power-curve model [Jaeger 1971] for small-scale shear strength. A separate adjustment is used for large-scale undulations (waviness). One advantage of this approach is that waviness is much easier and faster to measure in the field than are the types of data associated with the JRC method.

### Shear strength model

A general power-curve model for shear strength has been adopted for use in these programs. This curve is given by the following expression:

$$\tau = a\sigma^b + c, \tag{1}$$

where  $\tau$  =  shear strength,
$\sigma$  =  effective normal stress,
and  $a, b, c$  =  model parameters.

This equation describes a general power model with a y-intercept. It reduces to a simple linear model (Mohr-Coulomb failure envelope) when b equals 1.0, in which case, c is equal to cohesion and a is equal to the coefficient of friction (that is, $\tan\varphi$).

When using this model of discontinuity shear strength, a design engineer should beware of applying a linear (c, φ) failure envelope to the pseudo-residual shear data provided by a laboratory testing program. A linear model may seem appropriate for a large range of normal stresses (and may suffice for values exceeding 30 t/m² for most rock types), but such is not the

case for many natural discontinuity surfaces subjected to low values of normal stress. For example, the five shear data points presented in figure 10 are fit by a power model. A linear model is fit to three tests with the least normal stress, and a linear model is fit to all five tests. The results vary widely for the low normal stresses encountered near a bench crest.

Finally, time must be considered. Safe slopes are required only for as long as mining continues beneath these slopes. Likewise, the final pit slope generally is required to be stable only for as long as it takes to mine the last portion of the ore and get all personnel and equipment out of the pit. However, there are also cases where permanent structures or property lines are
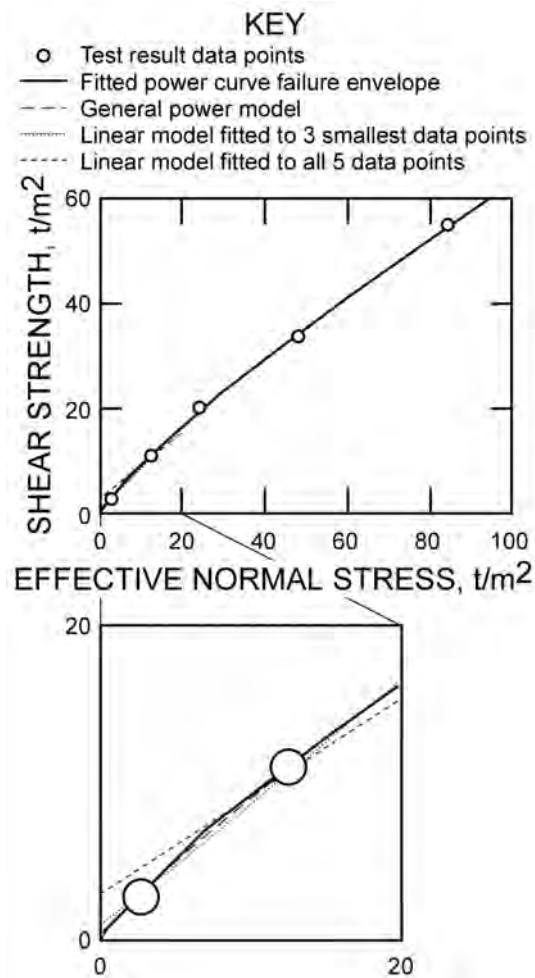


Figure 10. Power and linear models fit to test results at low normal stresses.

close to the top of the slope. These may require more conservative estimates of fracture shear strength.

### Waviness

The power curve model of strength is based on small samples and thus does not incorporate any resistance to sliding contributed by undulations or waviness on larger scales (roughly 1 to 10 m). Waviness can be quantified by measuring the average and minimum dips along the rock discontinuity(ies) of interest as part of collecting field data [Call et al., 1976]. Waviness is then defined by the relationship "waviness = average dip - minimum dip" and is expressed in degrees (figure 11). The tangent of this angle is multiplied by normal stress and added to shear strength resistance along the failure path.
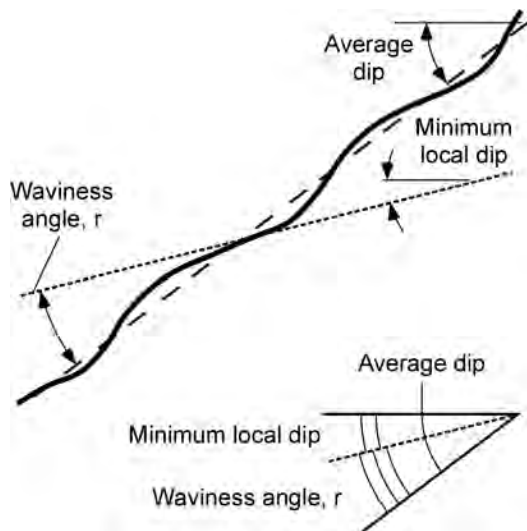


Figure 11. Waviness angle "r" of fracture surface.

The rationale for this adjustment is essentially geometric. The average dip of a sliding surface along a fracture is used to calculate the volume of a rock mass likely to fail (which leads to subsequent determinations of its weight and the effective normal stress acting on the fracture) and to resolve forces that act on the block in question. However, as a block begins to slide, it tends to detach from the steeper portions of the fracture and rest on portions with the flattest dip. This strength adjustment is analogous to changing fracture dip, but only for purposes of calculating resistance to slip. Thus, the greater the waviness, the greater the resistance to sliding.

### Shear strength variability

Variability in shear strength for a given normal stress is also considered. Shear strength is modeled with a gamma probability density function. The standard deviation of this function is defined directly in Bplane and Bstepp and by a coefficient of variation (CV), which is given by—

$$CV = s_\tau / m_\tau \qquad (2)$$
$$\text{or} \quad s_\tau = CV(m_\tau),$$

where $s_\tau$ = standard deviation of the shear strength ($\tau$) distribution
and $m_\tau$ = mean of $\tau$ given by Eq. 1.

Therefore, both shear strength mean and standard deviation increase with increasing normal stress. Typical values for shear strength CV range from 0.15 to 0.35. Note that for small values of CV (less than 0.2), the gamma probability density function begins to approximate a normal probability density function. The key advantage in using a gamma function to describe shear strength is that this particular function is defined only for positive values, which means that $\tau$ in the computer analysis can never take on a negative value.

The contribution of waviness (r) to shear strength is represented by an exponential probability density function, which makes the variable tan(r) have a right-skewed exponential-like probability density function. Implementation of the strength model in computation of probability and sliding is discussed by Miller et al. [2004].

# DETAILED PROGRAM DESCRIPTION

The Bplane, Bstepp, and Bwedge programs were designed to extend block slope stability analyses to incorporate statistical descriptions of fracture sets, including spatial correlations of important parameters. Thus, geostatistical descriptions are required for many input parameters. Specification of back failure lines on the bench (all programs) and face simulation lines (in Bwedge) is also required. These artificial constructs discretize the problem for solution, much like elements in a finite-element model.

The programs are written for personal computers (PCs) with Intel-compatible processors and all versions of the Windows operating system. Each program consists of a single, self-sufficient executable file compiled in the Lahey Fortran 95, version 5.5, programming environment. Since the programs require modest resources, they should run on most PCs. The run time for these programs is quite fast, almost always less than 5 min, depending on problem discretization and the number of iterations specified.

Two versions of each program are provided. The first version (Bplane, Bstepp, and Bwedge) is designed for intractive use with single sets of values. This requires a minimum of file handling and is good for exploring software capabilities. For sensitivity studies, a batch-processing version of each program is provided. Input files can be edited directly with a text editor or a utility program. Utility programs written for Microsoft Corp.'s Visual Basic 5.0 are provided for processing input files for batch versions of each program. Source code is also provided to enable users to further customize these utilities to their convenience.

Installation requires only that files are copied from the disk to a folder on a PC. The software is organized into three main subdirectories called "Programs," "Batch Input," and "Visual Basic Source." The Programs subdirectory contains executable files for the interactive version of each program. The Batch Input subdirectory contains versions of the program that are optimized for batch processing, along with file processing programs. The Visual Basic Source subdirectory contains source files for the Visual Basic programs. These should be useful to users who wish to automate file generation further.

## BPLANE.EXE
### (TWO-DIMENSIONAL PLANE SHEAR ANALYSIS)

Input for Bplane includes a description of bench geometry, rock properties, characteristics of a fracture set striking roughly parallel to the bench, and solution parameters. Bench geometry is described by height, width, and slope angle. Density is the only intact rock property required and is treated as a constant. Fracture characteristics length, dip, spacing, waviness, and strength are assumed to be described by appropriate statistical distributions. Length is modeled within the bench cross section as varying randomly within an exponential probability density function (where the standard deviation equals the mean). The dip direction of the fracture set should closely parallel dip direction of the slope face (within $\pm20°$). Fracture dip angles can vary spatially as described by a spherical variogram model as well as randomly. Fracture spacing is modeled by an exponential probability density function, and waviness is modeled by a skewed right beta probability density function (P=1,

---

[4]Mention of specific products and manufacturers does not imply endorsement by the National Institute for Occupational Safety and Health.

[5]Microsoft Corp., Redmond, WA.

Q=4). Small-scale fracture strength (on the scale of laboratory tests) is modeled as a power-curve failure envelope. Additional frictional resistance related to large-scale fracture geometry is modeled as fracture waviness.

## BSTEPP.EXE
### (TWO-DIMENSIONAL STEP-PATH ANALYSIS)

Input parameters for Bstepp include bench geometry, rock properties, characteristics of master and cross-joint sets, and solution parameters. Bench geometry is described by height, width, and slope angle. Fractures are characterized by length, dip, spacing, and strength. Fracture strength is modeled as a power-curve failure envelope defined by small-scale laboratory tests. Additional large-scale frictional resistance is provided by fracture waviness. Fractures are assumed to have strikes roughly parallel to the bench crest and be sufficiently long that out-of-plane termination of these fractures has little or no effect on the analysis. Unlike the preceding Bplane program, intact rock bridges between fractures are not automatically considered to stabilize the failure plane. Bridges are checked for tensile failure as part of the step-path failure surface. Thus, required rock properties include intact rock tensile strength as well as rock mass density.

Fracture input in Bstepp is required for both the master joint and cross-joint fracture sets. The master joint set intersects the face of the slope while the cross joint set is steeper and connects fractures of the master set. Where simulated cross joints fail to complete a path, intact rock bridges are included in the stability calculations.

Most of these parameters are allowed to vary within statistical distributions. These parameters include fracture characteristics (with the exception of length), but density is considered constant. Fracture dips can vary spatially as well as randomly, as described by a spherical variogram model defined by dip nugget, standard deviation (sill), and range. Fracture spacing can also vary spatially as well as randomly, but is modeled by an exponential geostatistical model. Waviness only applies to the master joint set, because cross joints will pull apart, not slide, during failure. A spherical variogram model is used to account for the spatial dependence commonly found in these parameters.

## BWEDGE.EXE
### (THREE-DIMENSIONAL WEDGE STABILITY ANALYSIS)

Input parameters for Bwedge are bench geometry, rock properties, characteristics of fracture sets that form each side of a failing wedge, and solution parameters. Bench geometry is described by height, width, and slope. The parameters for fracture dip, fracture dip direction, etc., are defined for both the left and right failure planes. One of the more common errors in using this program is input of failure planes that do not form a wedge and intersect the slope face (figure 12). Note that the left and right planes are defined as looking from the pit floor rather than from the slope crest (that is, left and right are viewed by looking up the intersection line).

Fracture characteristics are allowed to vary in accordance with various statistical distributions. Fracture dip angles (modeled with a normal probability density function) vary ac-
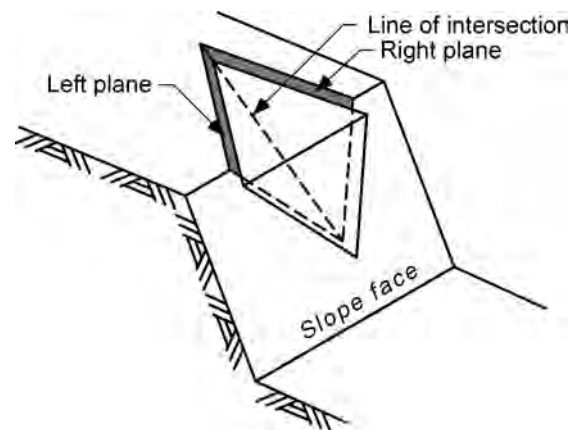


Figure 12. Viable wedge failure with daylighting intersection showing position of left and right failure planes.

cording to spatial dependence as described by a spherical variogram model defined by dip nugget, variance (sill), and range. Fracture spacing and waviness are simulated using an exponential probability density function. Mean fracture lengths in both sets are used to define the exponential probability density functions used to calculate the probability that fractures are of sufficient length to create a fully detached block.

## RUNNING THE INTERACTIVE VERSION

- *Start-Up*. Double-click executable file icon, and an input window will appear. The Bplane window is shown in figure 13, the Bstepp window in figure 14, and the Bwedge window in figure 15. A shortcut can also be created for execution from the desktop.

- *Parameter Input*. Enter the parameters necessary to run an analysis by simply clicking within the boxes and editing the values. Alternatively, the Tab key can be used to toggle to consecutive input boxes. Box-by-box definitions of input parameters are provided in appendix H. The specified units must be used. Example values are initially set in the boxes and can be used to test program operation. Boxes labeled "Sum. Results" will contain partial output from a run. Values need not be entered in these boxes and will not be considered during program execution if they are entered. The input screen specifies particular metric units for each parameter. Calculations and checks for appropriate input values are set specifically for these units. Other units or systems of units cannot be used.

- *Running Simulations*. When the desired parameters have been entered, click the "Compute" button to execute a simulation. The program may show "Not Responding" in the applications window of the task manager during execution, but soon a new window will appear saying that the program is computing.

- Each simulation examines potential failures resulting from a simulated set of discontinuities in the bench. Results will be unique to the random seed and number of simulations specified. However, results should converge as the number of simulations increases. It is recommended that the maximum allowable number of simulations (200 for Bplane, 100 for Bstepp, and 200 for Bwedge) be used unless there are computational time constraints. At least 30 simulations (50 for Bstepp) are typically needed to provide "defensible" statistical results.

- *Saving Results*. Output from each run, including a full list of run input parameters, is saved in the file specified in the output file box on the input window. Subsequent runs using the same file name will overwrite the previous file. Input data only are also written to temporary (.tmp) files named after the respective programs. These files can be copied after program execution, if desired.

- An additional explanation of some of these parameters, as well as practical guidance on assigning their values, is provided in the section on "Geotechnical Program Input" and the appendices.

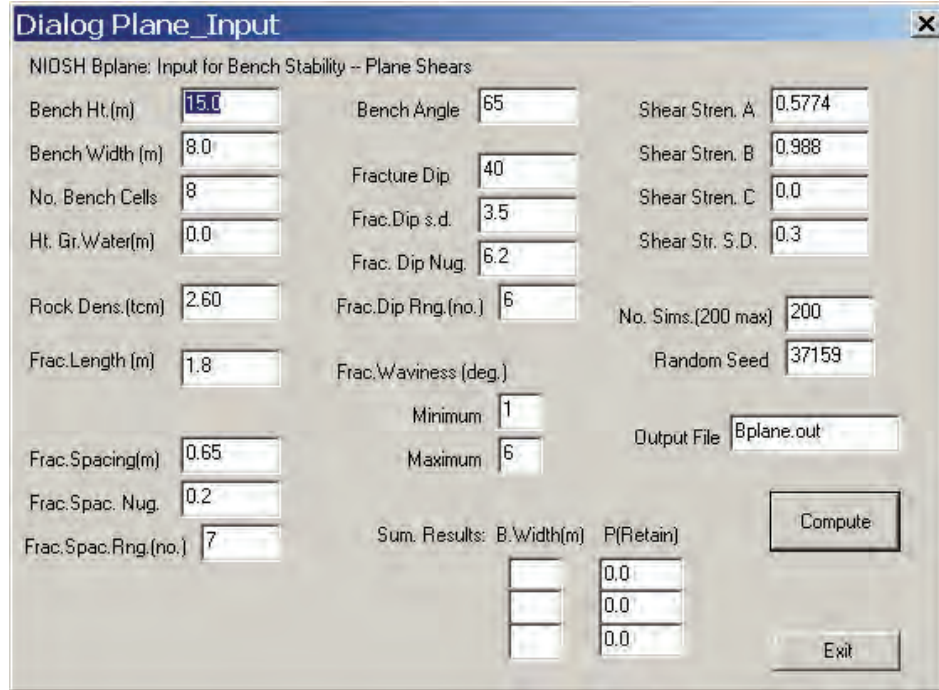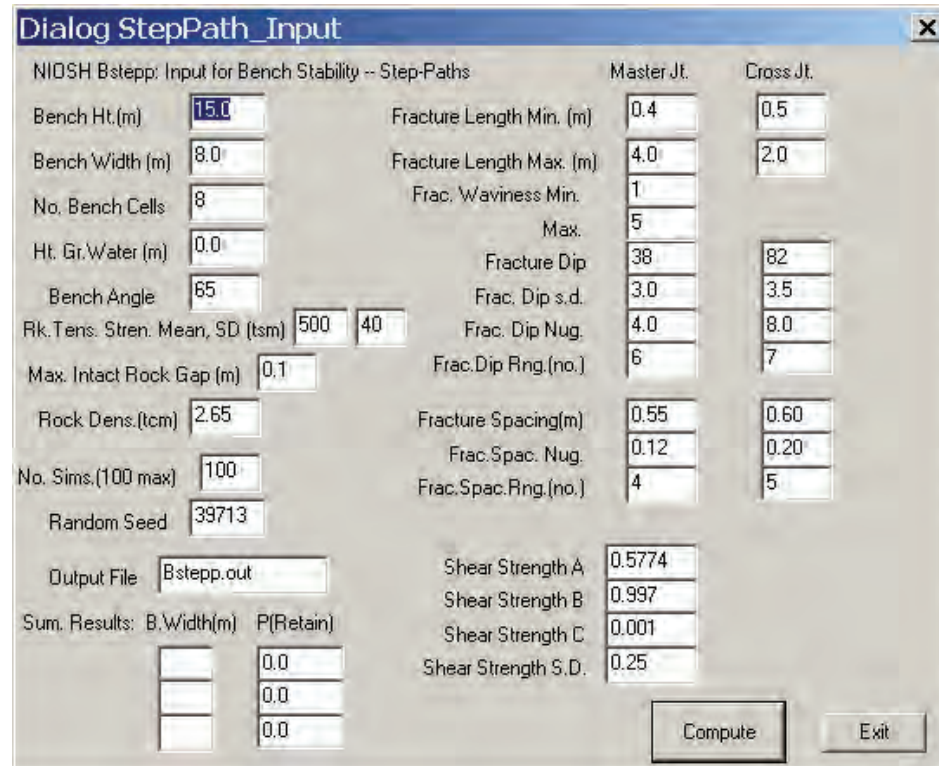Figure 13. Program window for Bplane



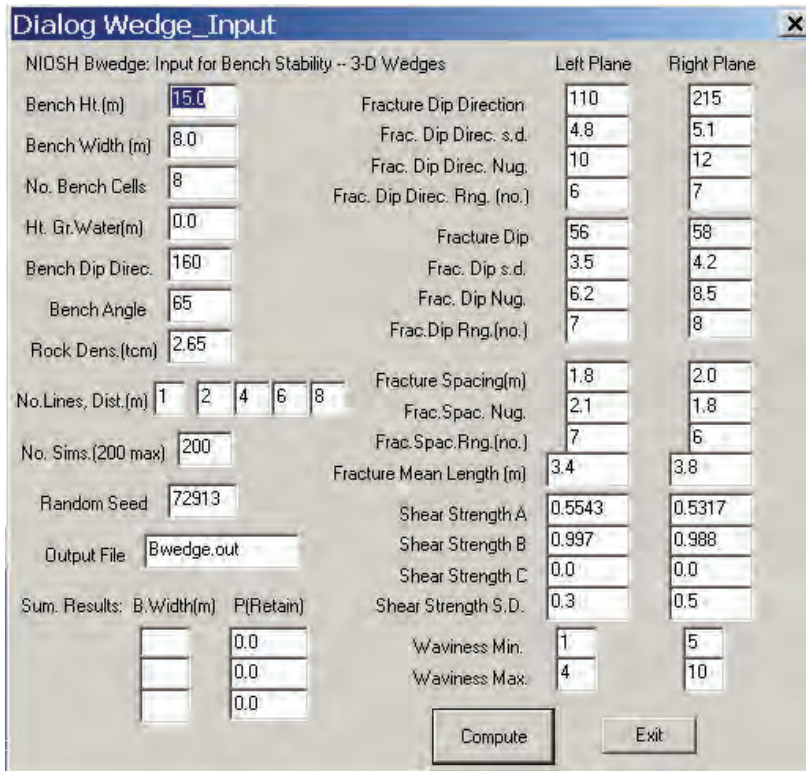Figure 14. Program window for Bstepp.

Figure 15. Program window for Bwedge.

## RUNNING THE BATCH VERSION

Application of the Bplane, Bstepp, and Bwedge programs to real problems often requires a sensitivity study to determine how results are affected by changes in various parameter values. Sensitivity studies can contribute significantly to a design. For instance, they can be used to identify critical input parameters that require extra attention during exploration. Sensitivity studies can also be used to check and refine input data over sections of an excavated bench where predicted and realized failures can be compared. This is a particularly valuable approach for developing confidence in program results. Sensitivity studies help engineers understand how benches are likely to perform under a wide range of design alternatives, thus supporting design optimization. Finally, apparently optimal designs can be tested for robustness, that is, sensitivity to reasonable errors in various parameters. A design that is hypersensitive to uncertain geologic variables introduces considerable risk compared to one that is more robust.

Batch processing versions of the three programs are included in a separate subdirectory along with related preprocessors. Program names are modified with a final "b" for "batch" (Bplaneb, Bsteppb, and Bwedgeb). The preprocessing programs InPlane 1.0, InStepPath 1.0, and InWedge 1.0 have interfaces that resemble the stand-alone programs, but are designed merely to read and write input files. They also can enable a switch (not accessible in the interactive version of the programs) that allows advanced users to bypass screening of input data. This allows analysis of data sets containing a wider variety of parameter values, but will also allow implausible data sets to be run, some of which may crash the programs.

Each of the batch programs assumes a particular input file name (bplaneb.inp, bsteppb.inp, bwedgeb.inp) and then writes to a file name specified in the input file. A controlling batch file (control.bat) can be used to rename each input file to the default name and then execute the program. The input file name is stored within the file to aid in tracking large numbers of runs.

In a typical application, a large number of input files having unique names would be generated. These runs might differ by small changes in one or more parameters. The input files could be generated by the preprocessing programs or by using a simple text editor (for example, Notepad or Wordpad, supplied with Windows). A control batch file is written that renames an input file, initiates the corresponding run, and then proceeds to the next input file. One batch file can execute a large number of runs, possibly requiring several hours of total run time.

Users may further optimize the preprocessing programs by modifying the Visual Basic code provided or by writing their own versions in a convenient programming language.

## INTERPRETATION OF OUTPUT

Results are reported as the probability that various bench widths will be retained for the specific failure mode being analyzed (that is, a particular failure mechanism involving a particular set of features). The probability of actually retaining a particular bench width will be the joint probability of individual probabilities calculated for each failure mode. Joint probability is calculated by multiplying individual probabilities. In the case of wedge failure, the probability gives the odds that any section of bench as long as it is high will not contain any failures that reach deeper

into the bench width than a particular value. In other words, the proportion of bench segments that lose a calculated width somewhere along that segment will be 1 minus the joint probability of retention. For example, a 0.80 probability of retaining 4-m-wide catch benches can be interpreted as an expectation that 80% of a long bench run will retain a width of at least 4 m and that 20% of the bench run will not.

The probability of losing all the bench is also an important consideration. In addition to eliminating any capacity for catching loose material, such a failure could undermine overlying benches, leading to larger scale failure. Thus, the design of overall slope angles should provide for very high probabilities (greater than 0.95) of retaining a bench of at least nominal width.

Results are typically plotted as a curve relating the probability of retaining bench width versus actual bench width at various bench face angles. Since bench geometry has a direct influence on the overall slope angle, similar plots can be made for overall slope angle (figure 16). The relationship between bench geometry and over-all slope angle can be expressed as follows:

$$\tan(A) = 1 / [(W/H)+(1/\tan B)], \qquad (3)$$

where
| | A | = | overall (average) slope angle, |
| | B | = | bench-face angle, |
| | H | = | vertical height of bench, |
| and | W | = | horizontal width of bench. |

For example, if H = 15 m, W = 8 m, and B = 64°, then A = arctan{1/[(8/15) + (1/tan 64°)]} = 44°.

If an overall steeper angle is desired, then the width:height ratio of benches must be decreased or the bench faces cut at a steeper angle. Relationships between bench geometry, catch-bench width, and over-all slope angle can be displayed in graphs, which then can be used to optimize bench slope angle and width for a
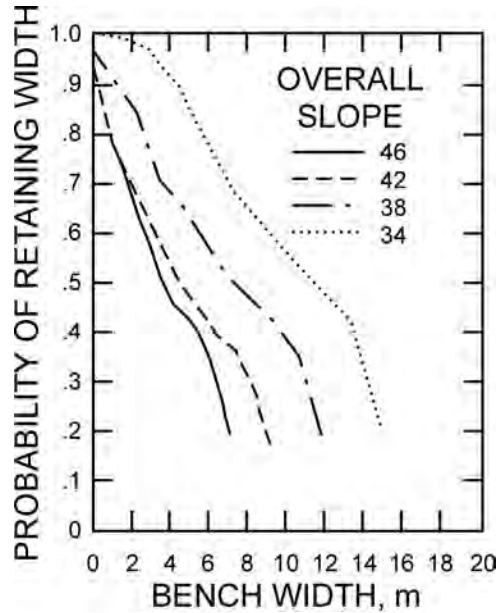


Figure 16. Typical results showing probability of retention for various bench widths and slope angles (calculated for plane shear failure, bench face angle of 64° (0.5:1), and bench height of 15 m).

specified probability of retaining a specified catch-bench width.

A key issue in interpreting output from this, or any, model of slope stability is the robustness of the result. A robust result from an engineering analysis is one that is not overly sensitive to a small change in input conditions. This is particularly important for analyses such as slope design that are largely dependent on estimates of inherently variable geologic conditions. For this reason, analyses should be conducted with reasonable ranges of critical parameters rather than with single, best-estimate values. The validity of estimates for the most sensitive parameters should be reviewed and design recommendations possibly refined.

For instance, fracture length (persistence) is often a critical parameter. Major geologic structures such as faults or contacts that are long enough to affect overall pit slope stability should be directly integrated into the slope design. Smaller (shorter) and more numerous fractures can be stabilized by intact rock bridges at scales larger than the bench. A small change in fracture

persistence can dramatically impact the range of block sizes that can fail. Small values for fracture persistence will limit failure to the crest lip. The step-path failure mode is an exception because it allows for a nearly continuous failure surface comprised of multiple fractures, each one of which may be short relative to the overall failure surface.

Care should also be taken to recognize what these results do not address. They do not predict how much of the failure will occur during excavation. Likewise, they do not reflect the influence of blasting practices, weathering, or additional loading from loose material or machinery placed on the bench to clean loose material. Finally, no allowance has been made for tension cracks that may truncate the failure paths. Thus, stochastic results may be approximate.

## SUMMARY

Computer software for a PC platform has been developed for stochastic analysis of bench stability in rock slopes. The computer programs analyze the potential for plane shear, step-path, and wedge failures along the bench crest and calculate the probability of retaining specified widths on affected catch benches.

Field studies are underway to evaluate and demonstrate how this software can be applied to mine pit slopes. These studies will be published and posted on the NIOSH web site along with updates to the software and software documentation. Users of this software are invited to contribute their experiences and suggestions. The full potential of this software depends on developing a body of experience, including case studies, with real-world application to the design of catch benches.

The software was developed to support safe mining in open pits and quarries where benches are used to catch material moving down slopes toward miners. The analyses may also be useful for other applications, including design of benches in civil projects.

# REFERENCES

Baecher GB [1980]. Progressively censored sampling of rock joint traces. Math Geol *12*:33-40.

Barton N [1973]. Review of a new shear strength criterion for rock joints. Eng Geol *7*:287–332.

Bridges MC [1976]. Fracture data for rock mechanics. Proceedings of the Second Australian-New Zealand Conference on Geomechanics. Brisbane, Australia, pp. 144–148.

Call RD [1972]. Analysis of geologic structure for open pit slope design. [Dissertation]. Tucson, AZ: University of Arizona.

Call RD and Nicholas DE [1978]. Prediction of step-path failure geometry for slope stability analysis. Unpublished paper presented at the 19th U.S. Symposium on Rock Mechanics, Stateline, NV, May 1–3, 1978, 8 pp.

Call RD and Savely JP [1990]. Open pit rock mechanics. Section 6.8. In: Kennedy BA, ed. Surface Mining, 2nd ed. Littleton, CO: Society of Mining Engineering, pp. 860–882.

Call RD, Savely JP, and Nicholas DE [1976]. Estimation of joint set characteristics from surface mapping data. In: Brown WS, Green SS, and Hustrilid WA, eds. Monograph on Rock Mechanics Applications in Mining. New York: AIME, pp. 65–73.

Call RD, Savely JP, and Pakalnis R [1982]. A simple core orientation technique. In: Brawner CO, ed. Proceedings of the Third Conference on Stability in Surface Mining. New York: Society of Mining Engineers, pp. 465–480.

Coates DF [1977]. Design. In: CANMET pit slope manual. Canada Centre for Mineral and Energy Technology. CANMET REPORT 77–5, p. 126.

Cruden DM [1977]. Describing the size of discontinuities. Intl J Rock Mech Mining Sci *14*:133–137.

Devore JL [1995]. Probability and statistics for engineering and the sciences. 4th ed. Belmont, CA: Wadsworth, p. 793

Einstein HH, Baecher GB, and Veneziano D [1978]. Risk analysis for rock slopes in open pit mines. Final report to the Bureau of Mines. contract no. J0275015.

Hoek E and Bray J [1981]. Rock slope engineering. 3rd ed. London: Institute of Mining & Metallurgy, p. 402.

International Society of Rock Mechanics [1977]. Suggested methods for the quantitative description of discontinuities in rock masses. Int J Rock Mech *15*:319–368.

Isiaaks EH and Srivastava RM [1989]. Applied geostatistics. New York: Oxford University Press, p. 561

Jaeger JC [1971]. Friction of rocks and stability of rock slopes. Geotechnique *21*:97–134.

La Pointe PR [1980]. Analysis of the spatial variation in rock mass properties through geostatistics. In: Summers DA, ed. Proceedings of the 21st U.S. Symposium on Rock Mechanics. Rolla, MO: University of Rolla, pp. 570–580.

Laslett GM [1982]. Censoring and edge effects in areal and line transect sampling of rock joint traces. Math Geol *14*:125–140.

Mahtab MA and Yegulalp TM [1982]. A rejection criterion for definition of clusters in orientation data. In: Goodman RE and Heuze FE, eds. Issues in Rock Mechanics. Proceedings: 23rd Symposium on Rock Mechanics. University of California, Berkeley, CA, Aug. 25–27. New York, NY: Society of Mining Engineers of AIME, pp.116–123.

Matheron G [1963]. Principles of geostatistics. Econ Geol *58*:1246–1266.

McMahon BK [1974]. Design of rock slopes against sliding on pre-existing fractures. Advances in rock mechanics. In: Voight B, ed. Proceedings of the 3rd Congress of the International Society for Rock Mechanics. Denver, CO, Sept. 1–7, Vol. 2, Part B. Washington, DC: National Academy of Sciences, pp. 803–808.

Meriam JL [1980]. Engineering mechanics. statics and dynamics, SI Version. New York: John Wiley and Sons, pp. 2:3, 2:15, 2:93.

Miller SM [1979]. Geostatistical analysis for evaluating spatial dependence in fracture set characteristics. In: O'Neil TJ, ed. Proceedings of the 16th International Symposium APCOM. New York: SME-AIME, pp. 537–545.

Miller SM [1982]. Statistical and Fourier methods for probabilistic design of rock slopes. [Dissertation]. University of Wyoming, p. 204.

Miller SM [1983]. Probabilistic analysis of bench stability for use in designing open pit mine slopes. Proceedings of the 24th US Symposium on Rock Mechanics. College Station, TX, pp. 621–629.

Miller SM [1984]. Probabilistic rock slope engineering. Vicksburg, MS: US Army Corps of Engineers, Waterways Experiment Station, Publication No. GL-84-8, p. 75.

Miller SM [2000]. Engineering design of rock slopes in open-pit mines based on computer simulations of bench stability. NIOSH contract report no. S9865708.

Miller SM and Borgman LE [1985]. Spectral-type simulation of spatially correlated fracture set properties. Math Geol *17*:41–52.

Miller SM, Whyatt JK, and McHugh E [2004]. Applications of the point estimation method for stochastic rock slope engineering. In: Yale DP, Willson SM, and Abou-Sayed AS. Proceedings of Gulf Rocks 2004: Rock Mechanics Across Borders and Disciplines, 6th North American Rock Mechanics Conference. June 5-10, Houston, TX: American Rock Mechanics Association.

Nicholas DE and Sims DB [2001]. Collecting and using geologic structure data for slope design. In: Hustrulid WA, McCarter MK, and Van Zyl, eds. Slope Stability in Surface Mining. Littleton, CO: Society for Mining Engineering, pp. 11–26.

Piteau DR [1970]. Geological factors significant to the stability of slopes cut in rock. In: Balkema AA, ed. Proceedings of the Symposium on the Theoretical Background to the Planning of Open Pit Mines with Special Reference to Slope Stability. Rotterdam, Netherlands, pp. 55–71.

Ristau JM [1994]. Field verification of a step-path simulation model for rock slope stability analysis. [Thesis]. University of Idaho, p. 134.

Robertson AM [1970]. The interpretation of geologic factors for use in slope stability. Proceedings of the Symposium on the Theoretical Background to the Planning of Open Pit Mines with Special Reference to Slope Stability. Johannesburg, South Africa, pp. 55–71.

Rosenblueth E [1975]. Point estimates for probability moment. Proceedings of the National Academy of Sciences. Vol. 72. No. 10. USA: National Academy of Sciences, pp. 3812–3814.

Ryan TM and Pryor PR [2001]. Designing catch benches and interramp slopes. In: Hustrulid WA, McCarter MK, and Van Zyl DJA, eds. Slope Stability in Surface Mining. Littleton, CO: Society for Mining Engineering pp. 27–38.

Shanley RJ and Mahtab MA [1976]. Delineation and analysis of clusters in orientation data. Math Geol $8$:9–23.

Terzaghi RD [1965]. Sources of error in joint surverys. Geotechnique $15$(3):287–304.

Zelen M and Severo NC [1965]. Probability functions. In: Abramowitz M, Stegon IA, eds. Handbook of mathematical functions. New York: Dover, pp. 925–995.

## APPENDIX A: KEY TERMS

*Design sector:* A region of a pit in which the most important parameters influencing slope stability are constant [Coates 1977]. These parameters include lithology, number and extent of discontinuities, rock mass properties, ore grade distribution, pit geometry (curvature), and operating factors such as the location of major haulage roads and crushers.

*Exponential probability function:* A special case of a gamma probability density function that is described entirely by its mean, which is equal to its standard deviation. The probability of occurrence declines exponentially from a maximum value to a value of zero.

*Failure:* Failure occurs when the loads or stresses acting on the rock material (intact or fractured) exceed the compressive, shear, or tensile strength of the rock or the strength of a plane of weakness or a discontinuity. Failure may result from destressing as well as stressing of a rock mass. For example, removing clamping normal stress along a discontinuity may induce sliding.

*Failure kinematics:* Failure kinematics is simply a geometrical description of the motion or movements that occur during a failure [Meriam 1980].

*Failure mechanism:* Failure mechanism is a description of the physical processes that take place in the rock mass as load increases and failure is initiated and propagates through the rock.

*Gamma probability function:* A flexible probability density function with no negative values that can take a range of shapes approximating the normal and exponential distributions at either extreme. The key advantage in using a gamma probability density function is that it is only defined for positive values. This property is particularly important for this application to the shear strength of geologic discontinuities.

Otherwise, the small normal stresses commonly encountered in analyzing small failed masses along bench crests would have a probability of creating a negative shear strength.

*Geostatistics*: A branch of applied statistics that focuses on the characterization of spatial dependence of attributes that can vary in value over space and the use of that dependence to predict values at unsampled locations.

Spatial dependence in fracture properties has been observed and can be described in geostatistical terms [La Pointe1980; Miller 1979]. Semi-variograms [Isaaks and Srivastava 1989] provide a statistical format for describing the spatial dependence of variabilities in fracture properties as a function of distance between fractures (figure A-1). The semi-variogram is defined by "nugget" (variance between neighbors), "sill" (variance between pairs of remote fractures), and "range" (distance at which variability reaches the sill value). Additional geostatistical background information is provided in appendix C.
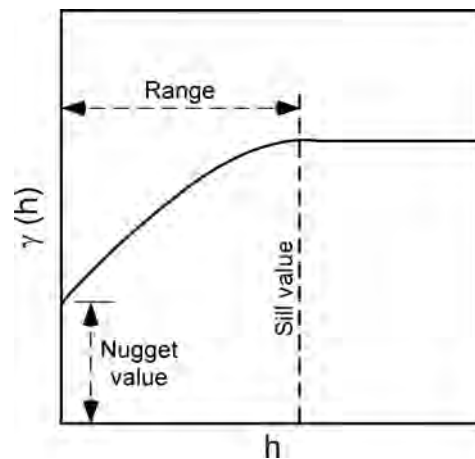


Figure A-1. Spherical semi-variogram model showing the variance in fracture properties as a function of distance between fractures (described by nugget, sill, and range).

*Joint set*: A group of rock joints that share a common or similar orientation (dip and dip direction). A joint set will appear as a cluster of points on a stereonet plot.

*Mean or expectation*: The mean (M[X]) or expectation (E[X]) of X is the centroidal axis of the probability density function of X. It is defined as—

$$M[X] = E[X] = \int_{all x} x f(x)\, dx. \qquad (A\text{-}1)$$

*Normal probability function*: A commonly used probability density function. The normal probability function is symmetric about the mean (figure A-2). The tails extend indefinitely, implying a vanishingly small probability of extremely high and low values (including negative values). To avoid problems with unusually high and low values, particularly the negative values for quantities such as strength and density, the probability density function is truncated in these programs by the addition of bounds at zero and ±4 standard deviations. Values generated beyond these bounds are set equal to the respective bound.

*Nugget*: The y-intercept on a variogram plot that corresponds to measurement error and short-scale natural variability in the spatial attribute of interest (figure A-1).
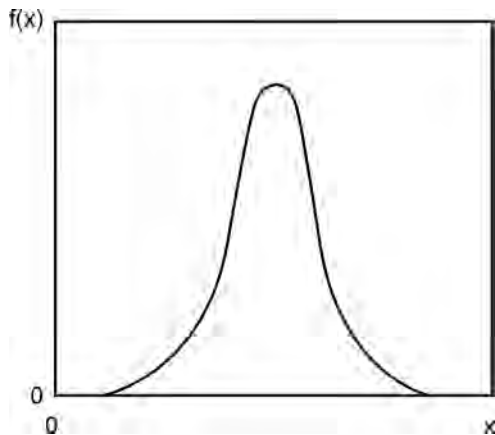


Figure A-2. Normal probability density function.

*Probability function*: A function that defines probabilities of occurrence for values of a random variable. Two common ways to represent such a distribution are cumulative distribution function and probability density function. The first describes the probability that a random variable will be less than or equal to a given value. The second is defined so that the area encompassed by the function is 1 and the area under the function between any two values represents the probability that a value within that range will be realized.

*Random variable*: A variable (that is, a mathematical entity used to model a physical property, attribute, or characteristic) that takes on different values when repeatedly sampled. These values cannot be predicted with certainty, but each value has an associated probability of occurrence. Random variables that are distributed over space are called regionalized variables. The overall relationship between values and probabilities is described by a probability density function. The term "random" as used here does not imply that the variable itself is random or has randomly distributed values, but rather that the values occur in a probabilistic manner. For example, a set of fractures can be regularly but imperfectly spaced. The variable of fracture spacing is not random, but there is some natural and measurement variability that prevents precise prediction of the spacing between two fractures.

*Range of influence*: The separation distance (lag) at which a variogram plot levels off; this represents the maximum distance at which the spatial attribute exhibits spatial dependence (figure A-1).

*Regionalized variable*: A type of random variable distributed over space. As such, it must be sampled over space at various locations. The distribution over space implies that variability between samples is a function of the position of

these samples relative to one another. Adjacent samples are likely to be more similar in value than samples distant from one another.

*Rock mass*: In situ rock material that includes blocks, discontinuities, and weathered and/or altered zones.

*Rock substance*: Solid, intact rock material that can be sampled and tested in the laboratory as a coherent piece.

*RQD (rock quality designation)*: The proportion of drill core length that is recovered in pieces longer than twice the core diameter.

*Semi-variogram*: A functional relationship between the separation distance (lag) between (1) two sampling locations (spatial attribute) and (2) the square of the average difference in value at two locations having the same (or similar) lag. For joint set attributes, this lag is measured in numbers of joints rather than in distance.

*Sill*: The variance for pairs of data points separated by sufficiently large distances to eliminate any spatial dependence.

*Standard deviation*: Standard deviation of a random variable X is the positive square root of the variance of X.

*Stochastic*: A synonym for probabilistic.

*Structural domain*: An area characterized by structures having a distinct pattern of orientation. These structures are mappable features such as fractures, bedding planes, and foliations. The identification of domain boundaries is essential to rock engineering investigations because geologic and hydrologic properties vary from one domain to another. Obvious domain boundaries are contacts between lithologic units caused by changes in depositional environment, intrusions, or fault displacement. However, domain boundaries may also occur within a rock unit and may be gradational.

*Variance*: Variance is a common measure of the dispersion (spread) of the random variable of X

about its mean. It is defined as—

$$\mathrm{var}[X] = \int_{alls} (X - M[X])\, f(x)\, dx. \qquad (A\text{-}2)$$

*Waviness*: Difference (in degrees) between the average dip of a fracture and the flattest dip observed along the fracture trace. Waviness accounts for the fact that the weight of a block tends to bear on the flattest portion of a fracture as movement begins. Geometrically, sliding movement will occur on flatter surfaces and will open gaps on steeper surfaces (in the absence of block rotation).

# APPENDIX B: MAPPING AND DISPLAY OF FRACTURE DATA[1]

Dominant geologic structures such as major faults and lithologic contacts are usually considered individually in rock slope engineering projects because they occur in definable locations and are continuous over distances comparable to the size of the study area. In contrast, structures such as fractures and foliations have high frequencies of occurrence and are discontinuous over a study area. They are too numerous to be mapped individually and, therefore, should be considered in a statistical manner.

## RATIONALE OF FRACTURE MAPPING

Geometric characteristics of fractures, including orientation, spacing, length, and waviness, are random variables that can be modeled by statistical distributions estimated from mapping data [Call et al. 1976]. Necessary fracture data can be collected by surface mapping techniques [Piteau 1970; Call 1972; McMahon 1974] and by oriented core logging. To map in detail every exposed fracture within a given area is impractical, if not impossible. Therefore, spot mapping is relied upon to provide a sample or samples of the fracture population from which distributions of the fracture properties can be estimated.

After a geologic mapping and evaluation program has been completed for the study area, a geologic map should be constructed to emphasize the rock units present, their contacts, and any major structures that may affect the stability of the proposed slope. This map, in conjunction with field knowledge of the area, provides the major basis for designing a fracture mapping program. At least one or two mapping sites are desired within each anticipated structural domain, and they should be located so as to help delineate and further define the domains. Careful thought and planning of the mapping program can not be overemphasized, because much time and money has been wasted by field sampling that has not been properly planned and directed.

If possible, the mapping samples should be random and representative so as to not make the population estimates biased or unrealistically weighted. Such samples are often difficult to obtain in the study area because surface outcrops are usually limited and biased toward the more competent rock materials. This sampling problem can be offset somewhat by mapping man-made cuts along construction or development roads and by oriented core logging of drill holes, even though such sites may be located for purposes other than fracture mapping and may have physical access limitations. Therefore, the slope engineer must remember that the interpretative step in estimating population parameters from sample data should be guided by subject-matter knowledge, experience, and judgment.

## EXAMPLES OF MAPPING TECHNIQUES

Many fracture mapping techniques are currently in use for collecting fracture data pertinent to rock engineering projects. The selection of mapping methods and styles primarily depends on the mapper's personal preference, site geology, size of the project, availability of mappable exposures, and the time and manpower allocated for the mapping task. However, most mapping schemes are variations of three fundamental techniques: fracture set mapping (or cell mapping), detail line mapping, and oriented core logging. Examples of these techniques that

---

[1]Excerpted from S. Miller, 1984, Probabilistic Rock Slope Engineering, Publ. No. GL-84-8, USAE-WES, Vicksburg, MS.

Figure B-1. Example of data recording sheet for fracture set mapping (from Rock Mechanics Division of Pincock, Allen & Holt, Inc., Tucson, AZ, 1979).

have been used extensively in rock engineering practice during recent years are described below. Suggested mapping forms (for example, field data sheets) that allow for rapid computer processing are also presented, but it should be remembered that variations or modifications may be required for individual mapping programs.

## Fracture set mapping

Fracture set mapping, which is also known as cell mapping, is a systematic method for gathering information about fracture sets and for helping to delineate structural domains. This mapping method is particularly valuable in situations where fracture data must be collected over a large area in a short period of time. It also provides information useful for evaluating variations in fracture patterns over the study area.

Natural outcrops and man-made exposures are located and identified as potential mapping sites. Long or extensive rock exposures are di-

vided into mapping cells of a regular, manageable size, usually about 8 to 12 m (approximately 30 ft) long. In each mapping cell, the dominant four or five fractures sets are recognized by locating groups of two or more approximately parallel fractures. Exceptionally large single joints and faults are also located; they will be mapped as single occurrences. Measurements of geometric characteristics and other information are then recorded for each fracture set or major structure in the cell.

An example of a field data sheet for recording fracture set mapping data is shown in figure B-1. Required basic information includes the project location, mapper's name, date, and an identification number for the particular area being mapped. At a given mapping cell or site, the following information is recorded on the illustrated data sheet for each fracture set or major structure.

*Coordinates*: The approximate map coordinates of the cell are recorded after being deter-

27

mined by map inspection, compass, and pacing techniques or surveying. These coordinates are repeated for each fracture set or major structure observed in the mapping cell.

*Rock type*: The rock type (or types) in the area being mapped is recorded with a three-letter alpha code.

*Structure type*: A two-letter alpha code is used to identify the type of structural feature being described. The most common code is "JS" for joint set.

*Structure orientation*: The overall average dip and azimuth strike of the fracture set are recorded using a right-hand convention whereby dip direction is 90° clockwise from strike direction. Orientation is identified by a two-number designation.

*Minimum dip*: The dip of the flattest fracture in the set is noted. For a single major structure, minimum dip is the dip of the flattest portion of its surface.

*Length*: The maximum traceable distance of the longest fracture in the set (or the single major structure) is recorded; this length is often limited by outcrop dimensions.

*Spacing*: The number of fractures in the set and the distance between the outer two, as measured normal to the fractures, are recorded to provide data for calculating mean fracture spacing. These measurements are not applicable to single major structures.

*Terminations, Roughness, Thickness, Filling, Water*: These data are recorded only for individual major structures. Descriptions of these measurements or observations are given in the section below on "Detail Line Mapping."

In a study area with accessible rock exposures, an experienced mapper can typically map a dozen or more cells per day. If possible, at least five or six cells should be mapped in each rock unit or suspected structural domain.

In remote areas with little or no construction and development, the mapping program should attempt to include most outcrops large enough to be mapped. By comparing fracture set data (especially orientation) from different mapping cells, the boundaries of structural domains may be better defined. Another major benefit derived from a thorough fracture set mapping program is that specific sites for collecting more-detailed fracture information can be identified.

## Detail line mapping

Detail line mapping is a systematic spot sampling technique for obtaining detailed information about the geometric characteristics of fractures and other geologic structural features. A measuring tape is stretched across the outcrop or exposure to be mapped. Using the tape as a reference line, a mapping zone is defined that extends 1 m above and 1 m below the line. The length of the mapping zone, or window, is determined by the complexity of the structural pattern, and accordingly, this length serves as a measure of fracture intensity. All structural features that are located at least partially in the zone are mapped, although a minimum length of 10 cm is typically enforced. That is, features with trace lengths less than this cutoff are not mapped. Experience has shown that a minimum of approximately 150 fracture observations per line is desirable for statistical evaluations [Call et al. 1976].

An example of a field data sheet for recording detail line mapping data is shown in figure B-2. Basic information recorded for each mapping site includes line identification number, location, data, mapper's name, bearing and plunge of the measuring tape, and attitude (orientation) of the rock exposure.

For each discontinuity within the mapping zone, the following information is recorded on the data sheet.

*Distance*: This is the distance along the measuring tape where the fracture or its projection intersects the tape. For any fracture parallel to the tape, the distance at the middle of the fracture trace is recorded.

*Fill*: Fill material (or materials) in the fracture opening is noted if present.

*Length*: Fracture length is the maximum traceable distance observed, which often extends beyond the mapping zone and is limited by outcrop dimensions. Lengths should be measured with a handheld tape, but longer fracture lengths (greater than approximately 3 m) may have to be estimated.

*Minimum dip*: Dip on the flattest portion of the fracture surface is recorded to compare with average dip. Their difference serves as a quantitative measure of fracture waviness.

*Overlap*: Overlap is the distance one fracture extends over the next fracture of the same set. For field mapping, the measurement is usually made along the trace length of each fracture and equals the distance from the bottom termi-nation to the mapping tape (figure B-3). If the fracture terminates below the tape, a minus distance is recorded. The true overlap can then be calculated later from the field measurements. Overlap is not applicable for fractures parallel to the tape.

*Parallel*: A fracture parallel to the measuring tape is designated by a letter P in this column.

*Rock type*: The rock type (or types) in which the fracture occurs is recorded by using a three-letter alpha code.

*Roughness*: Roughness is defined on a scale of centimeters and is a qualitative rating (smooth, rough, or medium) of small irregularities on the fracture surface. A numeric rating can also be used, such as that suggested by the International Society for Rock Mechanics [1977].

*Structure orientation*: Average dip and azimuth strike of the fracture are recorded using a right-hand convention whereby the dip direction is 90° clockwise from the strike direction. Fracture orientation is identified by a two-number designation.



Figure B-2. Example of data recording sheet for detail line mapping (from Rock Mechanics Division of Pincock, Allen & Holt, Inc., Tucson, AZ, 1979).
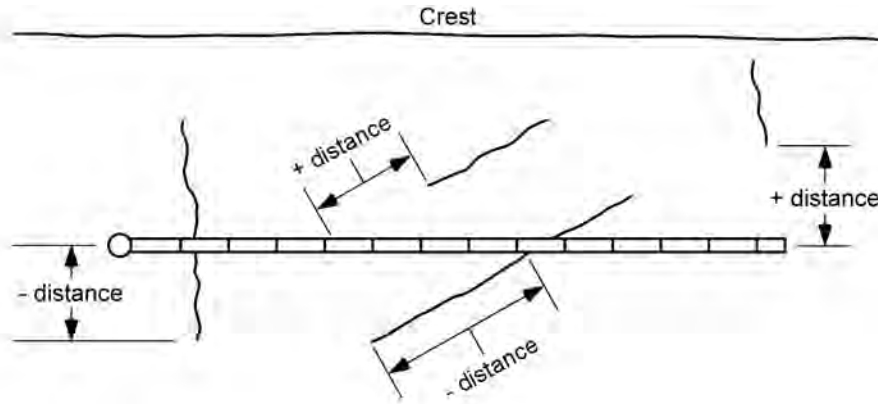
Figure B-3.—Illustration of field measurements for fracture overlap.



| T1 high angle > 20°<br>T2 low angle < 20° | T1 none<br>T2 none | T1 in rock<br>T2 in rock | En echelon |
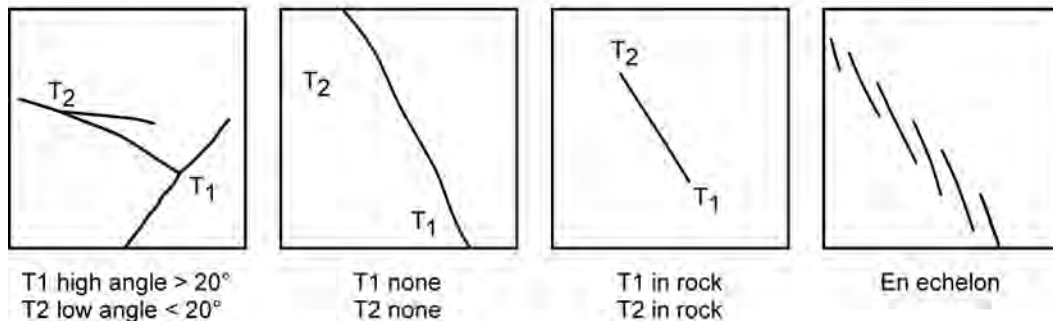
Figure B-4. Various types of fracture terminations.

*Structure type*: A two-letter alpha code is used to identify the type of discontinuity being described.

*Terminations*: The manner in which a fracture terminates is described by a single alpha letter according to five designations: in rock, none, en echelon, high angle against another fracture, and low angle against another fracture (figure B-4).

*Thickness*: Thickness is recorded if separation occurs along the fracture.

*Water*: The nature of water in the fracture (dry, wet, flowing, or squirting) is recorded using a single alpha letter.

For a typical mapping program in an area with accessible rock exposures, a team of two experienced mappers working together (one taking measurements, the other recording data) can usually map two or three detail lines per day. If possible, at least one complete line should be mapped in each structural domain preliminarily identified from available geologic information. Detail line mapping can not be feasibly used to cover as large an area as that covered by fracture set mapping, but it does provide a comprehensive base of detailed information that should be considered critical for statistical evaluations of fracture properties.

## ORIENTED CORE LOGGING

Subsurface fracture data can be obtained by oriented core logging, which provides a detailed record of fractures that intercept a diamond-drill hole. These types of data are similar to those of a very strict detail line survey in which only those fractures intersecting the line are mapped.

Figure B-5. Example of data recording sheet for oriented core logging (from Rock Mechanics Div. of Pincock, Allen & Holt, Inc., Tucson, AZ, 1979).



Figure B-6. Lower-hemisphere Schmidt plot of mapped fracture orientations obtained from a detail line site.

Various devices and systems are currently available for orienting structural features in core holes. The most popular and reliable of these are the Christiansen-Hugel system, the Craelius core orientor, and an eccentrically weighted clay-imprint orientor. The latter two devices can only be used in inclined drill holes. The clay-imprint orientor as described by Call et al. [1982] is by far the simplest, fastest, and least expensive device for orienting drill core. Its use has a small effect on regular drilling rates and costs, usually causing only a 10% to 20% decrease in rates and a corresponding increase in costs.

An example of a field data sheet for recording oriented core data from inclined drill holes is shown in figure B-5. Orientations of fractures in drill core are measured relative to the core axis and to a reference line that has been scribed or drawn along the top edge of the core by the orienting device. These field measurements are made with a specially designed goniometer and later converted to true dip directions and dips using vector mathematics and the drill-hole orientation.

For each fracture intercepted by the drill hole the following information is recorded on the illustrated data sheet.

*Angle to core axis*: Angle of the complement of dip angle relative to core axis.

*Circumference angle*: Azimuth measurement of dip direction of the fracture relative to the reference line.

*Depth from start*: The distance from the top of the drill run to the fracture occurrence is recorded. If 3-m drill runs are made this distance will always be less than 3 m.

*From – To*: Distances (depths) from the drill-hole collar to the top ("from") and bottom ("to") of the core run.

*Rock type*: The rock type (or types) in which the fracture occurs is recorded by using a three-letter alpha code.

*Structure type*: A two-letter alpha code is used to identify the type of discontinuity being described.

*Top/bottom*: A-B is recorded if the goniometer measurement is taken from the bottom end of a core stick; a T is used if the measurement is taken from the top end of a core stick.

*Roughness, Thickness, Filling*: These data are recorded only for individual major structures. Descriptions of these measurements or obser-vations are given in the section on "Detail Line Mapping."

Oriented core data are appropriately used to supplement surface mapping data because fracture lengths can not be measured in drill core. Another point to remember when analyzing core data is that measured fracture orientations tend to be more dispersed than those obtained from surface mapping. This is due to the fact that core diameter limits the fracture area that can be observed, and therefore very little averaging is done subsequently during the measurement process as compared to a fracture mapped in a surface exposure. Perhaps the greatest benefit of oriented core logging is a resulting database that allows determination of the sub-surface extent of the fracture sets and structural domains observed on the surface.

## DISPLAY OF FRACTURE ORIENTATION DATA

Before a suite of mapped fracture data can be statistically analyzed, fracture orientations must first be displayed so that fracture sets and structural domains can be determined. The orientations are plotted on lower-hemisphere projections that display poles to fractures. Schmidt equal-area projections are commonly used because pole densities can be readily calculated and then contoured to help enhance fracture patterns (figure B-6). The blind zone shown in figure B-6 corresponds to the orientation of the mapped outcrop where fractures that parallel the outcrop are overlooked or sampled to a lesser degree than fractures with strikes more perpendicular to the outcrop [Terzaghi 1965].

Schmidt plots derived from various mapping techniques are used in conjunction with knowledge of the local geology to help delineate structural domains in the study area. Fracture data are then combined within each domain,

and fracture sets critical to the slope design are identified. Geometric characteristics of the fracture sets can then be studied by generating histograms or cumulative distribution plots from which probability density functions can be estimated for the characteristics. These estimated functions are required for probabilistic evaluations and analyses of rock slope stability.

# APPENDIX C: INTRODUCTION TO GEOSTATISTICS AND VARIOGRAMS

One of the first issues requiring attention in a study of geostatistics is summarized in the following question: What is the difference, if any, between statistics and probability?

Statistics is the science that deals with the analysis of data and the processes of making inferences and decisions about the populations and/or systems from which the data were obtained. Thus, data are required for a statistical analysis. Examples of common statistical methods include describing confidence intervals for population parameters and comparing population parameters via the testing of hypotheses.

Probability is an internally consistent branch of mathematical logic based on systematic statements and the formulation of principles that allow descriptions of random variations in populations and/or systems to be made. Consequently, probability models can be constructed and used to describe and predict behavior or outcomes of sampling experiments based solely on professional knowledge and experience, and not necessarily on sampling data. Although data may be very helpful, they are not required for a probabilistic analysis. Examples of common probabilistic methods include descriptions of probability intervals, stochastic modeling and simulation, and hazard assessment.

Researchers and practitioners who deal with spatial populations and systems often ask the question: Given a set of data collected from a spatial population (for example, mining ore grades, soil or water chemistry, agricultural yields, etc.), how can the value at an unsampled location best be estimated?

In this instance, researchers are seeking a spatial estimate that can be obtained in several different ways. The most common are—

- Simple averaging of regional or local values. When knowledge of the spatial patterns of the attribute of interest is limited, the local mean is a reasonable estimate of the unknown value.

- Multiple regression or trend surface modeling (least squares, best fit) to describe a "best" surface passing through the cloud of data values mathematically. The estimated value at the unsampled location would be on this surface.

- Spatial interpolation via some defined algorithm that uses data in the spatial neighborhood (in proximity) of the unsampled location where the estimate is to be made.

## OVERVIEW OF GEOSTATISTICS

The field of geostatistics is not the application of statistics to geological or geoscience problems. Rather, the term has a more focused definition and much broader applications. Geostatistics is a branch of applied statistics that focuses on the characterization of spatial dependence in attributes that vary in value over space and the use of that dependence to predict values at unsampled locations. The notion of spatial dependence implies that two values from nearby locations will be more alike than two values from distant locations. Probably the closest relative to geostatistics is time-series analysis, wherein the time dependence of data is important for understanding and estimating an attribute that varies over time.

The amount of data needed for a geostatistical analysis that will lead to a spatial estimate is tied to several factors, the most important being the spatial configuration of sampling locations. Prudently located sampling sites can help reduce data requirements; however, in most

cases, a set of 25 to 30 observations is a realistic minimum. This would provide 300 to 435 pairs of values to be analyzed. The number of paired combinations for $n$ data points is $[n(n-1)]/2$.

Geostatistical tools can provide certain advantages over other spatial interpolation procedures provided there is an identifiable spatial dependence in the data set. Thus, adequate characterization of spatial dependence is essential for the proper implementation of geostatistical estimation procedures.

In recent years, the field of geostatistics has been expanded beyond spatial estimation to include probabilistic and stochastic procedures that lead to spatial simulations (sometimes known as stochastic images) of attributes. This provides another means to characterize, understand, and quantify uncertainties in mapping such attributes. Rather than being dubbed as "geoprobabilistics" or "geostochastics," these simulation approaches have simply been incorporated into the general collection of geostatistical tools available to knowledgeable workers who can select the right tool for the right job.

A typical geostatistical study consists of the following:

• Sampling design and data collection.

• Exploratory data analysis (plotting, graphing, univariate and bivariate statistical assessments, etc.).

• Analysis and modeling of spatial dependence (computation and plotting of spatial covariances and/or variograms, possible cross-validation to select desired models). Fitting of appropriate graphical models to the experimental variogram plots is often accomplished by subjective methods.

• Spatial mapping, which may consists of either or both of the following: (1) Spatial estimation via an interpolation method in the kriging family or (2) generation of spatial stochastic images via geostatistical simulation methods.

## EXPLORATORY DATA ANALYSIS

For any sampling program and subsequent statistical study, a reasonable number of observations is required for the attribute of interest. In a spatial analysis, an important attribute is the difference in sample value for pairs of observations at certain separation distances. To average such a difference or to make any statistical inference or estimate about this difference, an investigator must have a reasonable number of observed differences for each separation distance of interest. The only feasible way to obtain such a set of differences is to lump all sample pairs of a given separation distance as found across the entire study site. This lumping will force a careful consideration of the spatial character (particularly continuity, smoothness, and trend) of the physical property being sampled and estimated. Such is the goal of exploratory data analysis for spatial data sets.

## MAPS AND CROSS SECTIONS

One of the first investigations of a spatial data set should include map plotting of the values. Such maps include the following types:

• Post-plots or post-maps,

• Shaded-interval maps,

• Symbol maps,

• Contour maps, and

• Indicator-type shaded maps.

These maps clearly illustrate the continuity and sampling regularity (potential clustering) of the spatial attribute, as well as reveal the presence of any trends. In addition, the indicator maps show the spatial patterns associated with various cut-off values or thresholds that may be selected for the attribute of interest.

Cross sections or profiles can be constructed for specified directions where interesting features may be indicated by interval or contour maps. Fence diagrams also can be generated to connect one sampling location to the next if inadequate data are available along a straight line through the sampling region.

## MOVING-WINDOW STATISTICS

Once trends and discontinuities have been identified, basic exploratory data analysis calculations can be used to describe and help explain the spatial data set. If data are abundant, then subdividing the study site and analyzing (more particularly, averaging) over smaller areas is appropriate. However, if data are sparse, then one single area may be appropriate.

Neighborhood or local statistical estimates (most often the sample mean and standard deviation) can be computed using a moving-window scheme, provided there are adequate data for the study region. It is desirable to have at least four data points per window, but it is preferable to have at least six. An overlapping moving-window procedure is typically used to provide adequate numbers of local values.

Post-plots and accompanying contour plots of the local means and standard deviations can be helpful in the exploratory data analysis. For example, a contour map of the local means is a valuable tool for identifying and characterizing spatial trends in the data set, because much of the short-scale variability will have been smoothed out by local averaging. Also, by overlaying the contour maps of local means and standard deviations, heteroscedastic behavior (where variance is not constant across the site, but depends on local values) in the data set can be identified. Higher degrees of uncertainty about estimates in those local areas of high sample variance can be expected. Consequently, a contour map of local standard deviation values will highlight the local areas having high variability and thus

large estimation errors. These would probably be good places to collect additional data.

Scatterplots of local standard deviation versus local mean also reveal much about the spatial data set. For example, any significant relationship between the local mean and standard deviation indicates a proportional effect. Data that exhibit normal or Gaussian behavior typically do not have a proportional effect (that is, local standard deviation remains fairly constant across the site), whereas right-skewed data sets (for example, those that exhibit log normal behavior) often show a linear proportional effect.

Data transforms may be helpful for some exploratory data analyses. Highly skewed data have statistics that are influenced heavily by extreme values in the data set. One way to mitigate this influence is to use monotonous data transforms (that is, maintain the data ranks). These transformed values are used in subsequent computations, analyses, and estimates, then the results are reversed-transformed to complete the study. Examples of monotonous transforms include log, ln, rank, uniform-rank, and normal-score.

## LAG SCATTERPLOTS

An investigation of spatial dependence should include the generation of lag or h scatterplots (figure C-1). Such plots display pairs of values at specified lag separation distances in a given direction (if needed). Thus, as many lag scatterplots as there are lags and directions of interest can be produced. If the plotted points are tightly clustered about the 45° line on a given lag scatterplot, then significant spatial dependency is indicated at lag (h).

For typical spatial phenomena, this cloud of points becomes more dispersed as lag increases. In fact, the moment of inertia of such a point cloud about the 45° line can be computed and used as a measure of spatial de-
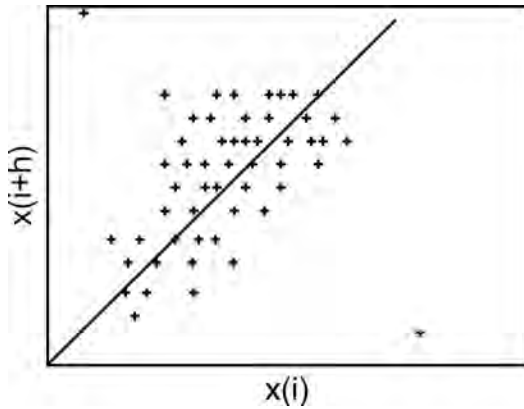
Figure C-1. Example of h scatterplot (lag scatterplot) for a specified lag (h).

pendence. A more dispersed cloud provides a greater moment of inertia and thus indicates less spatial dependence.

Lag scatterplots also provide a quick way to identify outlier pairs at particular lags and/or directions. Such pairs need to be recognized early in the spatial analysis because they can have significant impacts when spatial dependence measures are computed and spatial depen-dence models are fit. In many situations, removal of or ignoring certain outliers can be a major help in sub-sequent analyses of spatial dependence; however, in most cases, the outliers should be re-introduced to the data set before estimating and simulating the spatial attribute.

## SPATIAL DEPENDENCE

### Introduction

Recall the definition of the expectation operator for random variables:

$$E(X) = \int_{allx} x \cdot f(x)dx \qquad \text{(C-1)}$$

where  X  =  random variable,

f(x)  =  probability density function of the random variable,

and  x  =  value taken on by random variable X.

The expectation of a random variable is also know as the mean of the random variable.

When a random variable is used to describe (model) a spatial attribute, it must be indexed by location, and then it is known as a regionalized variable. If the location vector (x,y) is denoted as u, then a general regionalized variable pair can be written as X(u) and X(u+h) or a specific pair referenced to location ui can be written as $X(u_i)$ and $X(u_i+h)$. The two values at these two locations would be written $x(u_i)$ and $x(u_i+h)$.

The result is a pair of locations ($u_i$ and $u_i+h$) where h is the separation distance (lag) between the two locations. For many spatial attributes, pairs of regionalized variables are not indepen-dent, but are related by some type of spatial de-pendence. A shorter separation distance h often results in a greater dependence (figure C-2).

In a traditional statistical sense, many realiza-tions of the pair $X(u_i)$ and $X(u_i+h)$ are required to make statistical inferences. However, it is impractical to sample each location repeatedly just to get enough data for reliable averaging. Instead, averaging of pairs over the study re-gion must suffice; these pairs must be separated by a defined lag (h). Such global averaging forces some type of statistical stationarity as-sumption.

- Covariance stationarity: The mean does not depend on location, and the covariance for each pair of regionalized variables depends only on lag (h) and not on location. Data sets
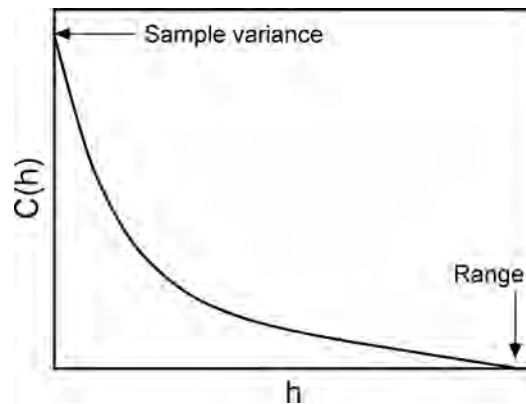


Figure C-2. Typical spatial covariance plot depicting spatial dependence.

that exhibit severe spatial trends are not suited for this model.

- Local stationarity: Covariance stationarity is re-stricted to local neighborhoods in which lag (h) is constrained by some defined limit.

Two common methods to deal with spatial data sets that exhibit regional trends are (1) to remove the trend, work with residuals to make spatial estimates, and add the trend back in and (2) to keep lag distances short in the spatial analysis and not extend estimates beyond well-defined local neighborhoods.

## Quantifying spatial dependence

One common way to describe the spatial dependence in a data set is to compute the sample spatial covariance, defined as—

$$C(h) = \frac{1}{n_h} \sum_{i=1}^{n_h} (x_i - \bar{x}_i)(x_{i+h} - \bar{x}_{i+h}) = \frac{1}{n_h} \sum_{i=1}^{n_h} x_i x_{i+h} - \bar{x}_i \bar{x}_{i+h}$$ (C-2)

where $x_i$ and $x_{i+h}$ = values separated by lag (h)
and $n_h$ = number of pairs separated by lag (h).

The notation for regionalized variable is—

$$C(h) = E\left[\{X(u_i) - m(X_i)\}\{X(u_{i+h}) - m(X_{i+h})\}\right] = E\left[X(u_i)X(u_{i+h})\right] - m(X_i)m(X_{i+h})$$ (C-3)

where $m(X_i)$ = mean of regionalized variable at lag-vector tails
and $m(X_{i+h})$ = mean of regionalized variable at lag-vector heads.

Another measure of spatial dependence can be related directly to the moment of inertia of the point cloud about the 45° line on any specified h scatterplot (recall figure C-1). If d is the perpendicular distance for a given point to the 45° line, then the moment of inertia I of the points about that line (figure C-3) can be written as—

$$I = \frac{1}{n} \sum_{i=1}^{n} d_i^2$$ (C-4)

However, we know that—

$$2d_i^2 = (x_i - x_{i+h})^2 \quad d_i^2 = \frac{1}{2}(x_i - x_{i+h})^2$$ (C-5)

This moment of inertia is known as the semi-variogram or variogram (figure C-4).

$$\gamma(h) = \frac{1}{2n_h} \sum_{i=1}^{n_h} (x_i - x_{i+h})^2$$ (C-6)

The notation for regionalized variable is—

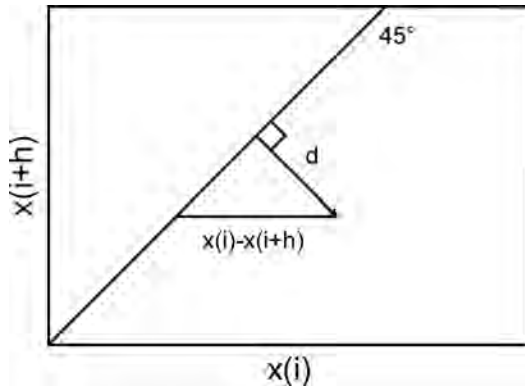$$\gamma(h) = \frac{1}{2} E\left[X(u_i) - X(u_{i+h})\right]^2$$ (C-7)

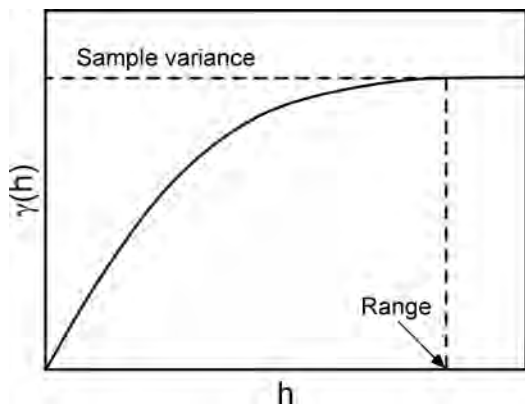Figure C-3. One point on a lag scatterplot to illustrate moment of inertia.



Figure C-4. A typical variogram plot depicting spatial dependence.

## Computational procedures

Two important guidelines should be considered when computing spatial covariance or variograms from a spatial data set.

1.  The number of data pairs per lag should always be more than 20, and usually be more than 30.

2.  The longest lag used in the computations should be no more than about 60% of the maximum lag available in the study region. This avoids the problems of under-sampling data locations in the middle of the site because long lag pairs have endpoints at the margins of the site.

For irregularly spaced points, the summations for lag pairs must incorporate cells, or bins, of specific distances. For example, all pairs having separation distances (lags) of 10 to 20 m would be grouped together into the 10- to 20-m bin and used to calculate one covariance value or one variogram value for that bin. The computed value is typically assigned to a lag equal to the mean lag of all pairs in that bin. If directional computations are desired, then the lag pairs must also be sorted by direction bins.

The lag bin boundaries are set arbitrarily by the investigator to obtain 6 to 20 bins, each having at least 30 pairs. For small data sets of $n < 25$, with the number of pairs $< 300$, it may suffice to have at least 20 lag pairs in the lag bins at shorter distances. Many variogram software programs give the user the flexibility to set all the lag-bin boundaries, so that the bins need not be uniform in size. Other programs only allow uniform lag bins.

Directional computations most often are referenced as east $= 0°$ and north $= 90°$, with directional bins being 15° to 30° in span. Typically, the initial calculations are set to 0°, 45°, 90°, and 135°, then a rough range ellipse is constructed to help discern the directions of longest and shortest spatial-dependence range. The range ellipse is then rotated and fine-tuned to provide a geometric model of anisotropy for the spatial attribute. The magnitude of the major and minor axes (two ranges) of the final ellipse and the direction of the major axis are identified for subsequent use in kriging (figure C-5).
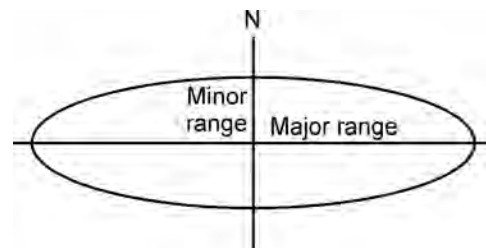


Figure C-5. Spatial-dependence range ellipse with major range at 0o (east-west).

### Valid variogram and covariance models

In many software packages, spatial covariance values are subtracted from sample variance to produce a complementary covariance (also known as inverted co-variance), which provides values and a plot shape similar to a variogram (figure C-6). Thus, even though the computational formulae are different for the covariance and the variogram, both the variogram and the complementary covariance can be fit to the same type of continuous models.

Because variogram structures can be combined in a linear combination, each of the following structures can be added to produce an overall model.

*Nugget effect*

$$\gamma(h) = \gamma_0 \text{ for } h = 0 \quad \text{(if } \gamma_0 = \text{ sample}$$
variance, then the result is pure nugget effect). (C-8)

*Spherical model*

Note that $h_r$ = range of influence; that is, the value of h for which spatial dependence disappears.

$$\gamma(h) = \sigma^2 \left[ \frac{3}{2}\left(\frac{h}{h_r}\right) - \frac{1}{2}\left(\frac{h}{h_r}\right)^3 \right]$$

for $0 \leq h \leq h_r$ (C-9)

or $\gamma(h) = \sigma^2$ for $h > h_r$.

*Exponential model*

$$\gamma(h) = \sigma^2 [1 - e^{-h/c}] \text{ for } h \geq 0 \quad \text{(C-10)}$$

The exponential model is similar to the spherical model except that it rises more steeply near the origin and has an effective range of $h_r = 3c$, where c is a constant. Note that $c = h_r/3$.

*Gaussian model*

$$\gamma(h) = \sigma^2 [1 - e^{-(h/c)^2}] \text{ for } h \geq 0. \quad \text{(C-11)}$$

A typical way to describe a variogram model is $\gamma(h) = 1.2 + 3.3\text{Sph}(52)$, where 1.2 is the nugget, 3.3 is the subsill (overall sill is 1.2+3.3 = 4.5), and 52 is the range.
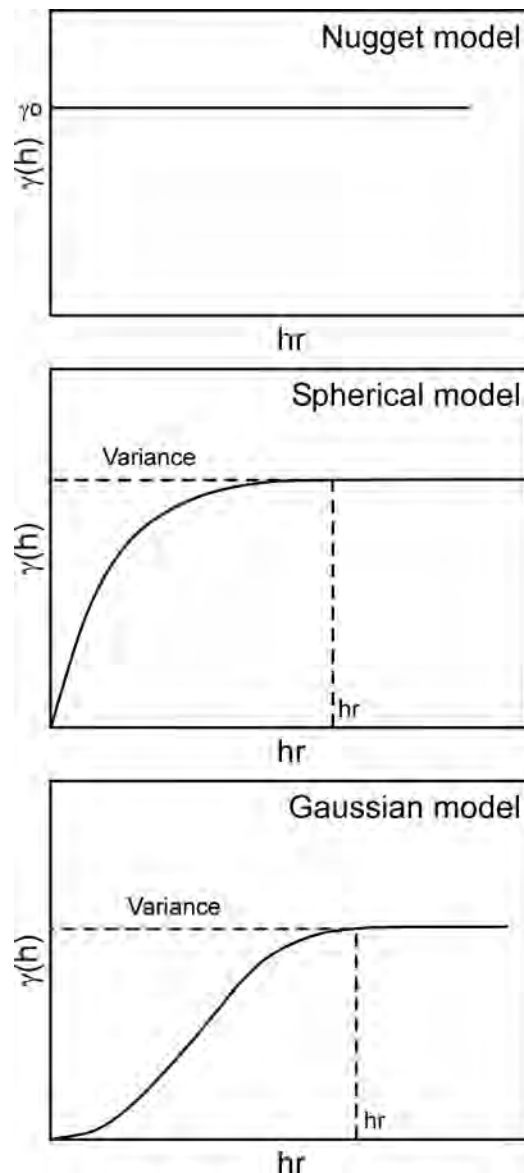


Figure C-6.—Three variogram models.

# APPENDIX D: STATISTICAL ANALYSIS OF FRACTURE DATA[1]

Mapped fracture orientations displayed on Schmidt plots provide the foundation for analyzing fracture data for probabilistic slope engineering. Plots obtained from various mapping sites are used to help delineate structural domains and to identify and describe fracture sets within each domain. After sorting the data according to sets, the fracture properties for each set are analyzed to obtain estimates of their probability distributions and spatial correlations.

## DELINEATION OF STRUCTURAL DOMAIN

The delineation of structural domain is essential to rock engineering studies because geologic and hydrologic properties vary from one domain to another. Obvious domain boundaries correspond to lithologic contacts caused by fault displacement, intrusion, or depositional environment. However, structural domain boundaries are not restricted only to lithologic contacts, but may also occur within the same rock unit. These less obvious boundaries often can be determined by visually comparing Schmidt plots that display fracture orientations from various mapping sites.

Preferred fracture orientations appear as clusters of poles on a Schmidt plot. Each cluster represents a fracture set, and the spatial relationships of clusters on the plot allow for meaningful visual comparisons with other plots. In the evaluation of two or more plots, geologic experience and judgment provide the basis for determining if the plots are alike and thus represent samples from the same structural domain.

If fracture orientations appear dispersed and random on the plots with no obvious clustering, then visual comparisons are not appropriate, and quantitative statistical methods are needed to evaluate the plots and provide guidance in locating structural domain boundaries. A chi-square test procedure has been adapted to the comparison of Schmidt plots and provides a way to evaluate confidence in claiming that two or more plots were obtained from the same structural domain [Miller 1983]. The procedure is based on the analysis of a contingency table (table D-1) that contains frequencies of fracture plots in corresponding patches on the Schmidt plots being compared.

In the contingency table, samples from r structural populations (domains) are listed down the rows in terms of the Schmidt plots. Each sample is classified into c categories, or patches. The frequency of observed fracture plots in the ij cell (i-th plot, j-th patch) is denoted by $f_{ij}$. To test the null hypothesis that the plots represent samples from like populations, the following statistic is calculated.

$$X^2 = \sum_{i=1}^{r} \sum_{j=1}^{c} \frac{(f_{ij} - e_{ij})^2}{e_{ij}} , \qquad (D-1)$$

where  r  =  total number of Schmidt plots,

C  =  total number of patches in each plot,

$f_{ij}$  =  observed frequency of fracture poles in the ij cell,

and  $e_{ij}$  =  expected frequency of fracture poles in the ij cell.

The expected frequency in the ij cell is calculated as—

$$e_{ij} = \frac{R_i C_j}{N} , \qquad (D-2)$$

where  $R_i$  =  total observed frequency of poles in the i-th row,

---

[1]Excerpted from S. Miller, 1984, Probabilistic Rock Slope Engineering, Publ. No. GL-84-8, USAE-WES, Vicksburg, MS.

$C_j$ = total observed frequency of poles in the j-th column,

and $N$ = total number of fracture observations in all plots.

If the null hypothesis is true, then the above statistic is chi-square distributed with $(r-1)(c-1)$ degrees of freedom (provided each fracture is sampled independently of other fractures), and its value does not exceed that of a chi-squared variant evaluated at a specified significance level $\alpha$. The value of $\alpha$ is actually equivalent to the area under a chi-square distribution to the right of its associated $X^2$ value. The usual test procedure consists of selecting an $\alpha$ value and then calculating the value of $X^2$ from the contingency table. The null hypothesis is rejected if this calculated value exceeds the known tabulated value of $X^2$ with $(r-1)(c-1)$ degrees of freedom for the specified $\alpha$.

Table D-1.—Arrangement of contingency table for comparing Schmidt plots

| Rows | Patch 1 | Patch 2 | Patch 3 | Patch c | Total |
|------|---------|---------|---------|---------|-------|
| Plot 1 | $f_{11}$ | $f_{12}$ | $f_{13}$ | $f_{1c}$ | $R_1$ |
| Plot 2 | $f_{21}$ | $f_{22}$ | $f_{23}$ | $f_{2c}$ | $R_2$ |
| Plot 3 | $f_{31}$ | $f_{32}$ | $f_{33}$ | $f_{3c}$ | $R_3$ |
| Plot r | $f_{r1}$ | $f_{r2}$ | $f_{r3}$ | $f_{rc}$ | $R_r$ |
| • | • | • | • | • | • |
| • | • | • | • | • | • |
| • | • | • | • | • | • |
| Column total | $C_1$ | $C_2$ | $C_3$ | $C_c$ | $N$ |

However, rather than selecting a particular significance level for comparing Schmidt plots, from a geologic standpoint, it is often desirable to use the calculated $X^2$ value from the continguency table to compute its corresponding right-tailed area $\alpha$. This computed $\alpha$ value is not really a level of significance, but serves as a measure of confidence in accepting the null hypothesis. It provides a quantitative and standardized measure of comparison among different contingency table analyses of Schmidt plots. A numerical procedure for estimating the right-tailed area under a chi-square distribution with more than 30 degrees of freedom is given by Zelen and Severo [1965].

In summary, contingency table analysis is a useful tool for comparing Schmidt plots and evaluating the alikeness of sampled structural populations. The method is intended for plots that display dispersed fracture orientations where the lack of well-defined clusters makes visual comparisons difficult and often times useless. The necessary statistical calculations can be easily programmed on a desktop computer, thus providing a rapid way to compare Schmidt plots obtained from various mapping sites. Such comparisons are important for helping to predict the locations of structural domain boundaries.

## COMBINING FRACTURE DATA FROM DIFFERENT MAPPING SOURCES

In fracture mapping programs for many slope design projects, various mapping techniques are employed at different sites. After structural domains have been delineated in the study area, the mapped fracture data can be combined by domain to provide a foundation for the statistical analysis of fracture set properties in each domain.

One of the first steps in combining fracture data is the delineation of fracture sets on each of the Schmidt plots. If fracturing is complex within a structural domain and preferred orientations are not readily seen in the plots, the density of fracture plots in small counting areas can be contoured to assist in the visual identification of fracture sets. Statistical methods are also available to help analyze and distinguish clusters of orientations on a given plot [Stanley and Mahtab 1976; Mahtab and Yegulalp 1982]. However, objective statistical analyses are strictly numerical and do not include engineering judgment that often make it possible to identify fracture sets from careful observations

of rock exposures. An experienced investigator who has mapped the fractures in an outcrop and has knowledge of slope design procedures and requirements can apply geologic information that is practically impossible for a statistical analysis to include. Therefore, statistical methods are tools that should guide, rather than control, delineation of fracture sets.

Because mapping methods and outcrop orientations often vary from one mapping site to another, observations of individual sets are analyzed separately to evaluate their characteristics. For instance, measured spacings in a given fracture set as mapped by detail line techniques are corrected to true spacings by using the mean orientation of the set and the orientation of the mapping line. This correction is different for each observation of the set (denoted as a subset) and for mapping line.

The mean vector of a mapped fracture subset is not only useful for the spacing correction, but also can be used to explicitly describe the mean orientation of the subset and aid in combining numerous fracture data obtained from different sites within a structural domain. This vector represents the average direction of normals to fracture planes in the given subset, and if plotted as a pole, it indicates the "center" of the Schmidt cluster that represents the observed fracture set. The normalized mean vector of a given fracture set is calculated by the expression below

where $\underline{V}_m =$  mean vector of fracture set,

$X_i, Y_i, Z_i =$  direction of a normal to the i-th fracture,

and  $N =$  total number of fractures in the set.

$$\underline{V}_m = \frac{1}{\sqrt{\{\sum_{i=1}^{N} x_i\}^2 + \{\sum_{i=1}^{N} y_i\}^2 + \{\sum_{i=1}^{N} z_i\}^2}} \begin{bmatrix} \sum_{i=1}^{N} x_i \\ \sum_{i=1}^{N} y_i \\ \sum_{i=1}^{N} z_i \end{bmatrix} \qquad (D3)$$

The plane orientation perpendicular to the mean vector is often truncated to serve as an abbreviated identifier for the fracture set. For instance, a mean vector plane with a dip direction of 162° and a dip of 47° would be labeled as 16.4. All the set mean vectors from different mapping sites within a given structural domain can then be plotted on a single lower hemisphere projection to aid in grouping fracture subsets (figure D-1).

Fracture set properties are combined directly if the same mapping technique was used for each subset in a given group. Thus, all the observations are pooled and treated as independent samples for calculating mean and standard deviation and for estimating probability distribution. However, if different mapping methods were used, then weighted means are calculated according to the number of fracture observations in each subset, and probability distribution are inferred from experience with other similar types of data. Selected fracture set properties taken from the data represented by figure D-1 are briefly summarized in table D-2.
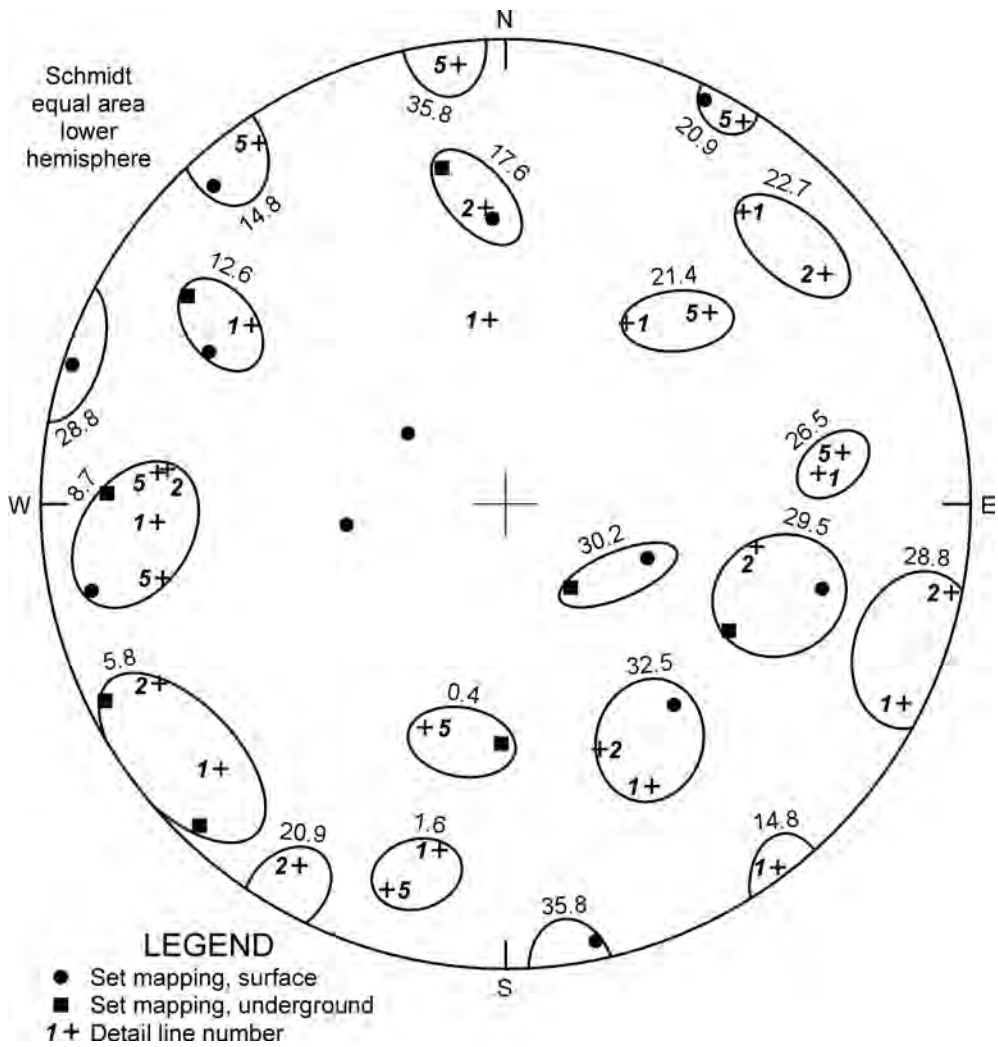
Figure D-1. Mean vector plot showing grouping of fracture subsets for a specified structural domain.

Table D-2.—Partial list of fracture set properties for structural domain represented by figure D-1

| Fracture set number | Number of observations | Dip direction, deg | | Dip, deg | | Length mean, m (ft) | Spacing mean, m (ft) | Waviness mean, m (ft) |
|---|---|---|---|---|---|---|---|---|
| | | Mean | S.D. | Mean | S.D. | | | |
| 0.4 | 23 | 5.7 | 9.7 | 42.6 | 8.2 | 0.76 (2.5) | 0.24 (0.8) | 0.70 (2.3) |
| 1.6 | 39 | 12.0 | 10.2 | 66.9 | 12.4 | 0.73 (2.4) | 0.15 (0.5) | 2.77 (9.1) |
| 5.8 | 56 | 50.9 | 9.7 | 82.6 | 10.2 | 0.98 (3.2) | 0.27 (0.9) | 0.94 (3.1) |
| 8.7 | 149 | 88.2 | 12.9 | 74.9 | 9.9 | 1.22 (4.0) | 0.34 (1.1) | 1.19 (3.9) |
| 12.6 | 30 | 122.9 | 10.8 | 67.3 | 11.6 | 0.94 (3.1) | 0.30 (1.0) | 0.12 (0.4) |
| 17.6 | 36 | 171.5 | 9.8 | 62.3 | 7.2 | 0.82 (2.7) | 0.27 (0.9) | 0.49 (1.6) |
| 26.5 | 25 | 261.0 | 8.4 | 61.3 | 15.0 | 1.43 (4.7) | 0.27 (0.9) | 1.28 (4.2) |
| 28.8 | 22 | 288.5 | 11.3 | 86.9 | 8.4 | 0.67 (2.2) | 0.43 (1.4) | 1.65 (5.4) |
| 28.5 | 134 | 291.3 | 9.8 | 52.2 | 12.5 | 1.04 (3.3) | 0.49 (1.6) | 0.46 (1.5) |
| 32.5 | 23 | 328.5 | 12.4 | 51.7 | 12.6 | 0.64 (2.1) | 0.21 (0.7) | 1.10 (3.6) |

## PROBABILITY DISTRIBUTION OF FRACTURE SET PROPERTIES

The combined fracture data for a given structural domain includes samples of fracture properties for all sets in that domain. These sample data can be used to construct histograms or cumulative frequency plots for pertinent properties in each fracture set. These plots are then used to help determine the probability density function that best describes the mapped fracture properties. Statistical goodness-of-fit tests can also be used in this evaluation process.

Distributions of dip and dip direction are usually best approximated by normal distributions (figure D-2), although some fracture sets may have orientation data that are nearly uniformly distributed. Distributions of set spacing, length, and waviness are typically approximated by exponential distributions [Robertson 1970; Call et al. 1976; Cruden 1977] as shown by the ex-
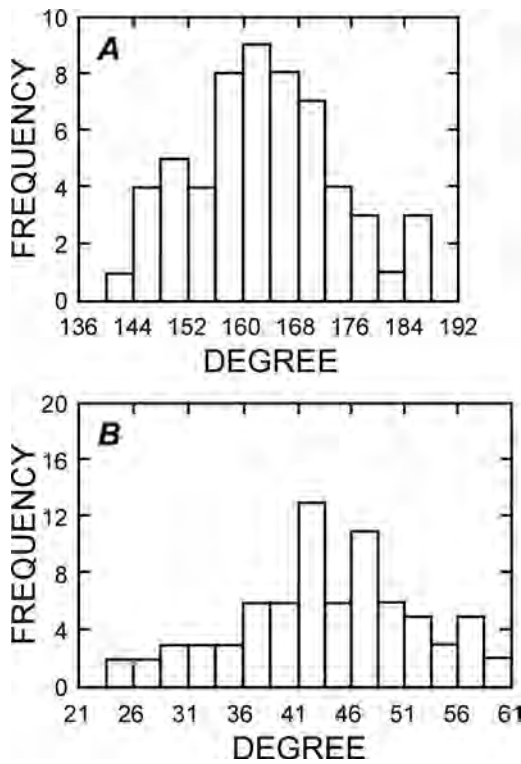
Figure D-2. Typical histograms of fracture set dip direction (A) and dip (B) that indicate normal distributions.
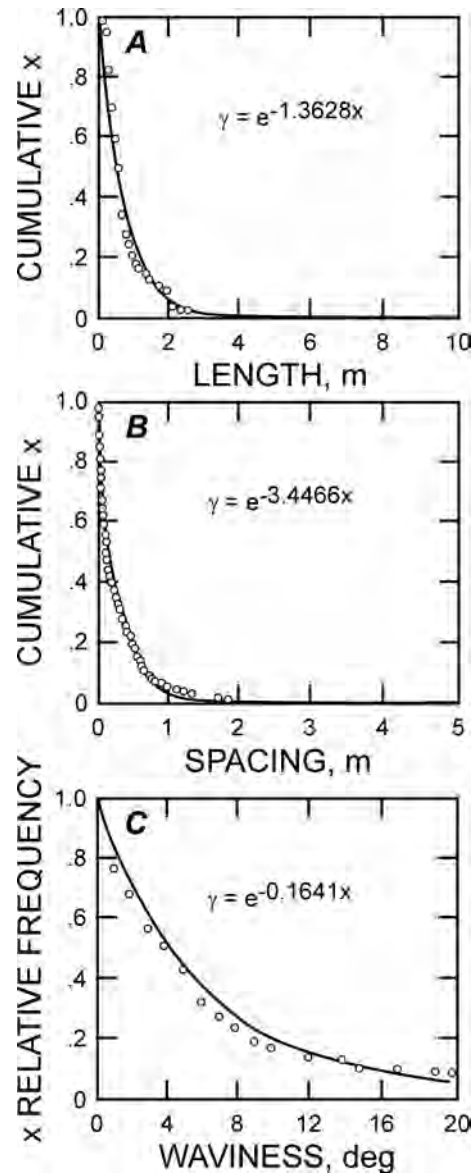
Figure D-3. Examples of exponential distributions of fracture set length, spacing, and waviness (from Call et al., 1976).

amples in figure D-3. However, some investigators report that trace lengths within a fracture set may be distributed in a log normal fashion [McMahon 1974; Bridges 1976; Einstein et al. 1978].

Statistical treatment of mapping bias and censoring of fracture length traces has been discussed by Baecher [1980] and Laslett [1982]. Such methods are used to adjust the distributions of mapped fracture lengths to provide im-

proved estimates of true length distributions.

Probability distribution forms other than those indicated above may occasionally be used to best describe the distributions of mapped fracture set properties. Regardless of which particular form is used, the basic requirements are that it be a valid probability density function that can be explicitly expressed and that it be amenable to subsequent slope stability analyses.

## SPATIAL CORRELATIONS OF FRACTURE SET PROPERTIES

A fracture property within a given set tends to be spatially correlated, and geostatistical methods can be used to determine the nature and extent of the correlation [Miller 1979; La Pointe 1980]. In classical statistics, the samples collected to describe an unknown population are assumed to be spatially independent (that is, knowing the values of one sample does not provide any information about adjacent samples). In contrast, geostatistics is based on the assumption that adjoining samples are spatially correlated and that the nature of the correlation can be statistically and analytically expressed as a variogram function [Matheron 1963].

In the analysis of fracture set properties, weak second-order stationarity is assumed, and estimates of variogram functions are computed along the mean vector line of each fracture set [Miller 1979]. A given variogram function is estimated from sample data along a line according to—

$$\hat{\gamma}(h) = \frac{1}{2N} \sum_{i=1}^{N} [Z(x_i) - Z(x_i + h)]^2 \qquad \text{(D-4)}$$

where $Z(x_i)$ = sample value at location $x_i$,
$Z(x_i + h)$ = sample value at location $x_i + h$,
and $N$ = total number of sample values.

The estimated function $\gamma(h)$ is expressed in a graph with h plotted as the independent vari-
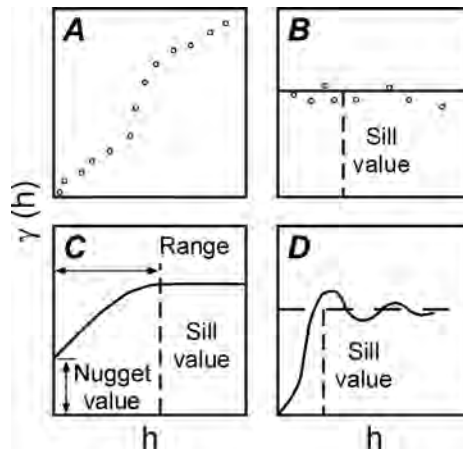


Figure D-4. Examples of variograms and theoretical models. A, Variogram showing high spatial correlation and continuity of samples. B, Variogram showing no spatial correlation of samples. C, Theoretical spherical model showing some spatial correlation of samples. D, Theoretical hole-effect model showing spatial correlation of periodic samples.

able. For fracture set data, distance h can either be measured in terms of actual distance or in terms of number of fractures. The number of samples used in estimating the function should be at least 30 in most cases.

Examples of variograms and theoretical variogram models are shown in figure D-4. For the spherical model, the value of $\gamma(h)$ at the point where the curve reaches a plateau is called the sill value, and the corresponding value of h is called the range. The sill value equals the variance of all sample values used in calculating the variogram. The range can be considered in the traditional geologic concept of range of influence (that is, any two samples spaced further apart than this distance are not spatially correlated). Thus, the variogram represents a measurement of correlation as distance between sample increases. Ideally, the nugget should be zero because any two samples from the same point should have equal values.

However, a nugget practically always occurs in variograms of geologic data and may indicate highly erratic sample values spaced close to one another or may reflect errors or uncertainties in sample collection and evaluation.

Typical variograms for fracture set properties are illustrated in figure D-5. For most fracture sets, the spherical model is appropriate for describing the spatial relationships of a specified fracture property. If periodicity is indicated, then a modified hole-effect model can be used [Miller 1979].
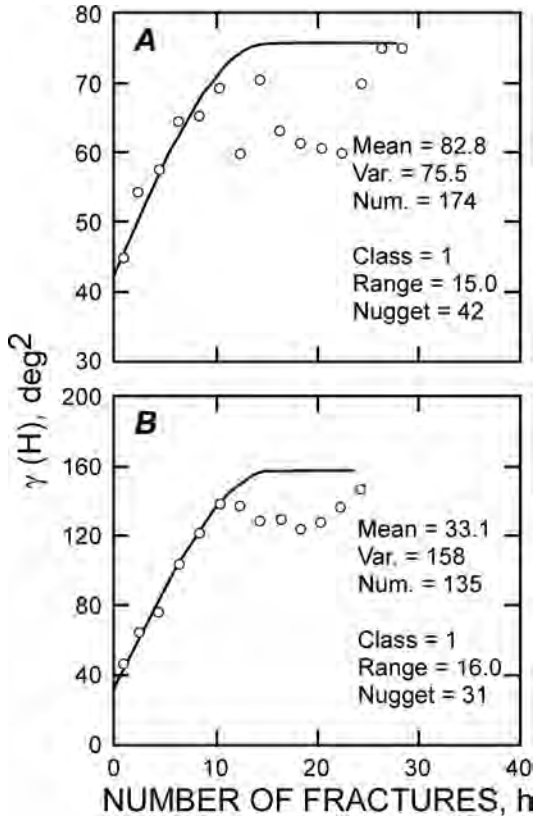


Figure D-5. Example variograms of fracture set properties (from Miller, 1979).

# APPENDIX E: EXAMPLE PLANE SHEAR ANALYSIS FOR BENCH DESIGN

Geotechnical fieldwork has provided the following field mapping data for a possible plane shear fracture set (actually, this set consists of relict bedding planes in a quartzite rock mass). Bplane calculations in this appendix were conducted with a beta version that contained different treatments of density and waviness.

## CASE 1

Consider a case where an overall slope angle of 53° and 8-m-high benches are desired. Thus, several combinations of bench width and face angle are investigated to provide the overall angle (68° at 2 m, 76° at 4 m, and 89° at 6 m). Recall the geometric relationship $(1/\tan\varphi) = (1/\tan 53°) - (W/8)$.

Step 1. Calculate and model the fracture set variograms for dip, waviness, and spacing based on mapping data (table E-1). This can be accomplished using various software programs. In this example, the demonstration version of Golden Software's Surfer8 was used. The results are illustrated in figures E-1, E-2, and E-3.

Step 2. Measure or estimate other rock mass properties needed for the analysis.

Rock mass density mean = 2.67 t/m³.
Rock mass density standard deviation = 0.02 t/m³ (not available in the release version).
Mean fracture length = 6.2 m.
Fracture shear strength:
A = 0.6249 (tan 32°).
B = 0.990 (a slight curvature from a linear model).
C = 0 (zero cohesion intercept.)

Step 3. Execute the program Bplane and summarize bench back-break results. Sample input and output are shown in figures E-4 and E-5. The results are summarized in tables E-2 and E-3.

Note that the probability of retaining a 2-m-wide catch bench is quite low in all three configurations, reflecting the long mean length (6.2 m) of the fracture set. The preferred engineering design option likely is to not bench at all, but to have the cut slope coincide with the natural fracture set for the finished slope.

Table E-1.—Sample data set

| Count | Spacing (to next fracture) | | Dip direction | Dip | Dip, mean | Waviness | Length, m | Tape, ft |
|---|---|---|---|---|---|---|---|---|
| | Feet | Meters | | | | | | |
| 1 | 0.19 | 0.058 | 57 | 46 | 44 | 2 | 7.6 | 5.90 |
| 2 | 0.53 | 0.162 | 36 | 52 | 49 | 3 | 7.2 | 6.19 |
| 3 | 0.27 | 0.082 | 53 | 44 | 42 | 2 | 7.3 | 7.00 |
| 4 | 0.49 | 0.150 | 54 | 44 | 41 | 3 | 7.7 | 7.41 |
| 5 | 0.68 | 0.208 | 60 | 43 | 39 | 4 | 7.0 | 8.16 |
| 6 | 0.92 | 0.281 | 55 | 46 | 42 | 4 | 7.2 | 9.20 |
| 7 | 0.10 | 0.030 | 62 | 44 | 39 | 5 | 6.9 | 10.60 |
| 8 | 0.43 | 0.131 | 58 | 44 | 40 | 4 | 7.0 | 10.75 |
| 9 | 0.31 | 0.094 | 53 | 48 | 45 | 3 | 6.7 | 11.40 |
| 10 | 1.17 | 0.357 | 62 | 41 | 37 | 4 | 6.9 | 11.87 |
| 11 | 0.39 | 0.119 | 70 | 40 | 37 | 3 | 6.4 | 13.65 |
| 12 | 2.07 | 0.631 | 62 | 43 | 40 | 3 | 6.1 | 14.25 |
| 13 | 0.53 | 0.162 | 63 | 49 | 46 | 3 | 6.1 | 17.40 |
| 14 | 1.25 | 0.381 | 49 | 45 | 42 | 3 | 6.3 | 18.20 |
| 15 | 0.29 | 0.088 | 59 | 50 | 48 | 2 | 5.5 | 20.10 |
| 16 | 0.47 | 0.143 | 55 | 43 | 40 | 3 | 5.3 | 20.54 |
| 17 | 0.22 | 0.067 | 60 | 45 | 41 | 4 | 5.5 | 21.25 |
| 18 | 0.14 | 0.043 | 53 | 45 | 41 | 4 | 5.4 | 21.58 |
| 19 | 0.53 | 0.162 | 55 | 48 | 45 | 3 | 5.2 | 21.80 |
| 20 | 0.26 | 0.079 | 70 | 40 | 37 | 3 | 5.8 | 22.60 |
| 21 | 0.16 | 0.049 | 58 | 41 | 38 | 3 | 5.6 | 23.00 |
| 22 | 0.23 | 0.070 | 61 | 44 | 40 | 4 | 5.6 | 23.25 |
| 23 | 0.76 | 0.232 | 58 | 45 | 40 | 5 | 5.7 | 23.60 |
| 24 | 0.20 | 0.061 | 56 | 42 | 38 | 4 | 6.1 | 24.75 |
| 25 | 0.15 | 0.046 | 59 | 45 | 42 | 3 | 6.1 | 25.05 |
| 26 | 0.47 | 0.143 | 56 | 41 | 39 | 2 | 5.8 | 25.28 |
| 27 | 0.46 | 0.140 | 60 | 40 | 36 | 4 | 6.0 | 26.00 |
| 28 | 1.12 | 0.341 | 68 | 35 | 32 | 3 | 6.1 | 26.70 |
| 29 | 0.16 | 0.049 | 68 | 38 | 34 | 4 | 6.4 | 28.40 |
| 30 | 0.30 | 0.091 | 55 | 38 | 35 | 3 | 6.2 | 28.65 |
| 31 | 0.33 | 0.101 | 49 | 42 | 38 | 4 | 6.2 | 29.10 |
| 32 | 0.32 | 0.098 | 62 | 40 | 37 | 3 | 6.3 | 29.60 |
| 33 | 0.64 | 0.195 | 56 | 43 | 39 | 4 | 5.9 | 30.09 |
| 34 | 0.22 | 0.067 | 64 | 41 | 38 | 3 | 6.2 | 31.06 |
| 35 | 0.07 | 0.021 | 65 | 44 | 41 | 3 | 6.7 | 31.40 |
| 36 | 0.32 | 0.098 | 69 | 44 | 42 | 2 | 6.7 | 31.50 |
| 37 | 0.36 | 0.110 | 64 | 40 | 38 | 2 | 6.6 | 31.99 |
| 38 | 0.53 | 0.162 | 58 | 43 | 40 | 3 | 6.5 | 32.54 |
| 39 | 0.21 | 0.064 | 67 | 44 | 42 | 2 | 7.0 | 33.35 |
| 40 | 0.68 | 0.207 | 41 | 42 | 40 | 2 | 6.6 | 33.67 |
| 41 | 0.72 | 0.219 | 54 | 44 | 40 | 4 | 7.2 | 34.71 |
| 42 | 0.29 | 0.088 | 56 | 38 | 36 | 2 | 7.3 | 35.80 |
| 43 | 0.05 | 0.015 | 65 | 42 | 39 | 3 | 7.5 | 36.24 |
| 44 | | | 57 | 40 | 36 | 4 | 7.2 | 36.31 |

Table E-2.—Summary of results for 8-m-high benches

| 68° and 2 m wide | | 76° and 4 m wide | | 89° and 6 m wide | |
|---|---|---|---|---|---|
| Width, m | Probability of retention | Width, m | Probability of retention | Width, m | Probability of retention |
| 2 | 0.064 | 4 | 0.039 | 6 | 0.019 |
| 1 | 0.163 | 3 | 0.089 | 5 | 0.039 |
| 0 | 0.312 | 2 | 0.183 | 4 | 0.083 |
| | | 1 | 0.314 | 3 | 0.149 |
| | | 0 | 0.465 | 2 | 0.248 |
| | | | 0 | 1 | 0.367 |
| | | | | 0 | 0.507 |

Table E-3.—Summary of results for 8-m-high bench with 2.2-m mean fracture length

| 68° and 2 m wide | | 76° and 4 m wide | | 89° and 6 m wide | |
|---|---|---|---|---|---|
| Width, m | Probability of retention | Width, m | Probability of retention | Width, m | Probability of retention |
| 2 | 0.010 | 4 | 0.296 | 6 | 0.223 |
| 1 | 0.151 | 3 | 0.550 | 5 | 0.405 |
| 0 | 0.494 | 2 | 0.767 | 4 | 0.622 |
| | | 1 | 0.893 | 3 | 0.769 |
| | | 0 | 0.950 | 2 | 0.873 |
| | | | 0 | 1 | 0.931 |
| | | | | 0 | 0.964 |

## CASE 2

Repeat the analysis shown in Table E-2, but assume a shorter mean length, for example, 2.2m.

Note that the probability of retaining a 2-m-high bench (Table E-3) increases significantly for the two steeper bench face angles. The preferred engineering design option here is to construct steeper benches. The 76° angle is probably better because it will produce less crest back-break material than will the 89° angle.
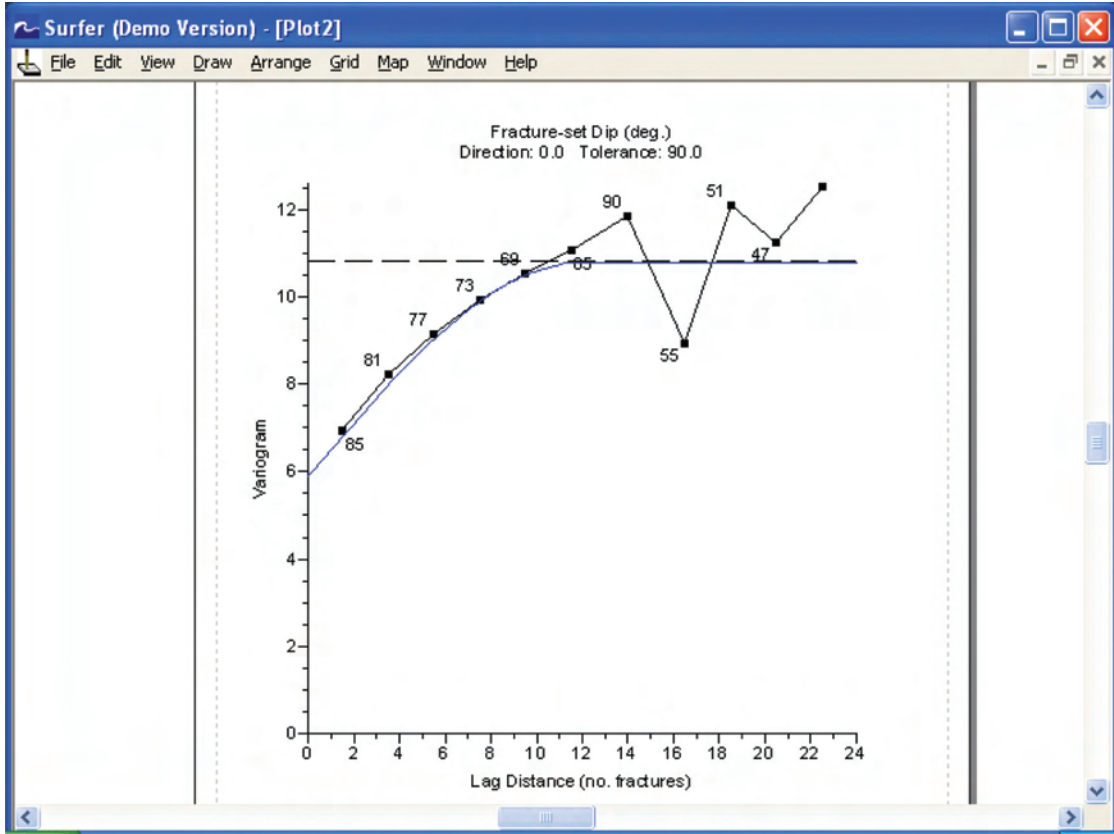
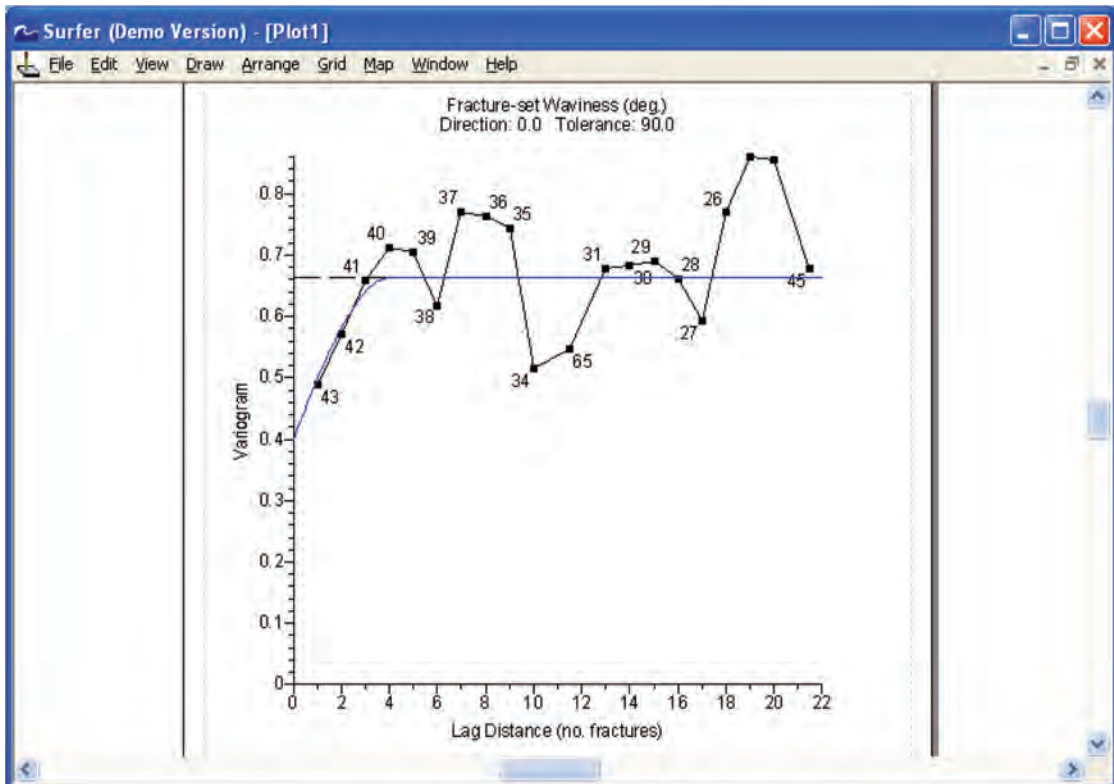Figure E-1. Estimated variogram and model for fracture set dip:   (h) = 5.9 + 4.9Sph(12).



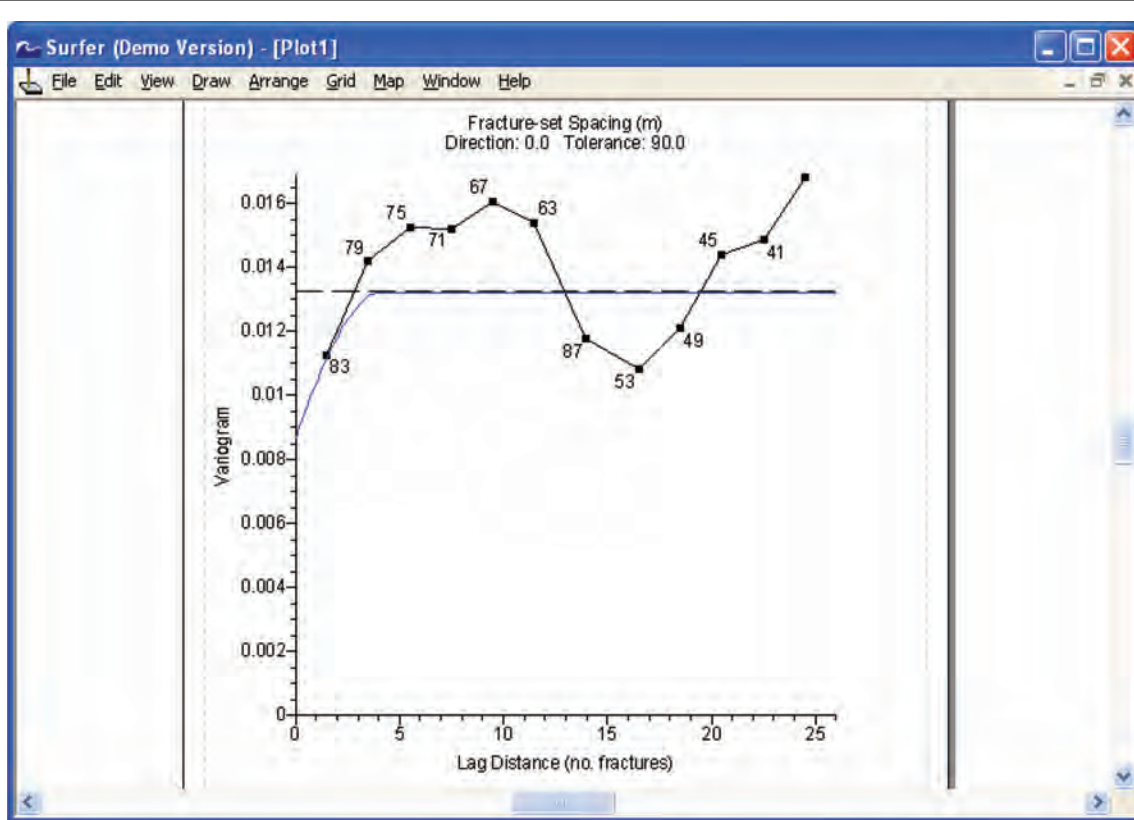Figure E-2. Estimated variogram and model for fracture set waviness:   (h) = 0.40 + 0.263Sph(4).

Figure E-3. Estimated variogram and model for fracture set spacing:  (h) = 0.0087 + 0.0045Sph(4).



Figure E-4. Example input screen and summary results for program Bplane (case 2).

```
Bplane76 - Notepad

File  Edit  Format  View  Help

NIOSH Bplane Output
Bench Simulation -- Plane Shear Analysis

Bench Ht. & Width (m)              8.00    4.00
Bench Face/Slope Angle (deg.)      76.0
Ht. Grd.Water from Toe (m)         0.00
Rock Unit Wt. Mean & SD (tcm)      2.670   0.020
Fracture Length Mean (m)           2.20
Fracture Spacing Mean (m)          0.11
            Nugget Value           0.009
            Range (no. frac.)      4.0
Fracture Waviness Mean (deg.)      3.2
            Nugget Value           6.18
            Range (no. frac.)      4.0
Fracture Dip Mean & SD (deg.)      43.0    3.3
            Nugget Value           5.90
            Range (no. frac.)     12.0
Gen. Shear Stren. Model:  tau =  0.000 + 0.6249sig^0.9900
    with CV = 0.200
No. Bench Simulations & Random Seed   150  37159.

Results of Analysis:

        BENCH        PROB. OF RETAINING
       WIDTH (m)       THE BENCH WIDTH

        4.00            0.29609
        3.00            0.54976
        2.00            0.76748
        1.00            0.89263
        0.00            0.94968
********************************************
```

Figure E-5. Output file of results for the Bplane example (case 2) given above in figure E-4.

# APPENDIX F: COMPUTATIONAL PROCEDURES

The computational procedures required for assessing whether a plane or wedge failure might occur under specific conditions are quite simple and can easily be programmed into a spreadsheet. Since fractures that cause failure in bench crests are often too numerous and too small to be mapped individually, they are mapped statistically and described by probability density functions. Probability density function input is then examined by using the same procedures as for specific conditions to generate a probability density function that describes the probability of failures that could compromise various bench widths.

The probability density function input is treated in different ways within the NIOSH bench stability codes. The first method involves a geostatistical spatial simulation of fracture set properties (spacing, dip, and waviness) to assign a realistic fracture pattern to the bench (see Miller and Borgman [1985], for more detail on the simulation procedure). The second method deals with shear strength along each potential failure path by using a spatial convolution of input probability density function to generate a safety factor; this provides an estimate of the probability of sliding [Miller 1982].

A discretization scheme that divides the bench width into cells is presented. Output probability results are presented for cell boundaries, which should be defined at critical dimensions. Then, an overview of the statistical procedures that are applicable to both computational approaches is provided. Finally, an outline of the specific computations programmed in Bplane is presented. Bwedge follows a similar procedure.

## BENCH BACK-BREAK CELLS AND STABILITY ANALYSIS

The concept of bench back-break cells is illustrated in figures 16 and 17 in the main text. For the plane shear analysis (figure 16), a ran-dom starting point is selected near the bench toe, after which fracture locations up the bench are simulated by generating spatially dependent fracture spacings. Fracture dip and waviness values also are generated using spatial dependence and assigned to individual fractures previously located on the slope face.

By simulating many realizations of a given bench, each of which contains multiple occurrences of the particular failure mode, the probability of stability for any specified back-failure cell can be estimated as follows [Miller 1983]:

$$P_{CS} = [(N_T - N)/N_T] + \qquad (F-1)$$
$$+ (1/N_T) \sum_{i=1}^{N} \left\{ \prod_{j=1}^{J_i} [(1 - P_{Lj})|_{Si} + \right.$$
$$+ P_{Lj}(1 - P_{Sj})|_{Si} \},$$

where $P_{CS}$ = probability of cell stability,

$\quad N_T$ = total number of bench simulations,

$\quad N$ = number of bench simulations having at least one failure path in the specified cell,

$\quad S_i$ = i-th bench simulation,

$\quad J_i$ = number of failure paths in the specified cell for i-th bench simulation,

$\quad P_{Lj}$ = probability of sufficient length for j-th failure path,

and $\quad P_{Sj}$ = probability of sliding for j-th failure path.

To simulate three-dimensional wedges in a bench, a standard length along the bench face must be specified to define an area for probability accumulations. This length is typically set equal to bench height to provide for square units that can be analyzed along the bench face

(figure 18). The number and size of simulation windows depend on fracture set spacings, lengths, and engineering judgment [Miller 1983].

## PROBABILITY OF STABILITY FOR SIMULATED FAILURE MODES

The probability of retaining a specified bench width for given failure modes in a bench can be estimated by simulating potential failure geometries and cataloging the back-break position of each one on the top of the bench. Stability of a given failure geometry can occur in two ways.

1. Failure length is not long enough to pass entirely through the bench and
2. Failure length is long enough to pass through the bench, but sliding does not occur [Miller 1983].

The probability of stability for each geometry then is given by the sum of these two probability values.

*Failure length is not long enough*

$$P_{stab} = P \qquad (F-2)$$
(failure path not long enough) +
P(failure path long enough and no sliding),
in which $P_{stab} = (1 - P_L) + P_L(1-P_S)$

where $P_L$ = probability that the failure path is long enough to extend through the bench

and $P_S$ = probability of sliding along the failure path.

Thus, the probability of failure length and the probability of sliding must be computed for each potential failure mass generated in the bench simulation.

*Failure length is long enough*

The probability that a given simulated fracture is long enough to pass entirely through the bench is computed as an exceedance probability using an exponential probability density function model for the fracture set lengths. The exponential cumulative distribution function is a one-parameter model given by Devore [1995].

$$F(x) = 0 \text{ if } x < 0, \qquad (F-3)$$
$$F(x) = 1 - e^{-x/m} \text{ if } x \geq 0,$$

where $m$ = mean.

The length required for a through-going failure path for a plane shear fracture is calculated by—

$$X = h_f/\sin(D), \qquad (F-4)$$

where $h_f$ = vertical height of failure mass (toe of failure to top of bench)

and $D$ = dip of failure plane (or wedge intersection line for wedge failures).

Thus, the probability that fracture length takes on a value greater than x is given by—

$$P(X > x) = 1 - P(X \leq x) \qquad (F-5)$$
$$= 1 - F(x)$$
$$= 1 - (1 - e^{-x/m})$$
$$= e^{-x/m}$$
$$= P_L.$$

For example, for a mean length of 1.6 m and x equaling 3 m, then $P(X > 3) = e^{-3/1.6} = 0.153 = P_L$.

In the case of three-dimensional wedges, which slide along the line of intersection, the probability of length sufficient for failure is the joint probability that the left fracture is long enough and the right fracture is long enough.

$$P_L(\text{wedge}) = P_L(\text{left}) \times P_L(\text{right}). \qquad \text{(F-6)}$$

After setting the length of the wedge intersection equal to $x$ in Eq. F-6, the corresponding $P_L(\text{left})$ and $P_L(\text{right})$ can be computed using mean length for the left fracture set and mean length for the right fracture set, respectively.

## PROBABILITY OF SLIDING

The probability of sliding for a given slope failure mode is evaluated by using the point estimation method [Rosenblueth 1975] applied to a limiting-equilibrium analysis in which the mean and standard deviation of a safety factor (F) are computed directly [Miller et al. 2004]. A gamma probability density function is assumed for F, and the probability of sliding ($P_S$) is computed by numerically integrating the area under this function to the left of $F = 1.0$. That is,

$$P_S = P(SF \leq 1.0). \qquad \text{(F-7)}$$

## OVERVIEW OF COMPUTATIONAL PROCEDURES USED IN THE BPLANE PROGRAM

The following computational steps are completed by Bplane for each bench simulation. Typically, the number of bench simulations will be between 100 and 150.

1.  The Fast Fourier Transform (FFT) method is used to simulate 256 spatially dependent, normally distributed values of fracture set **dip** for the identified plane shear fracture set. These 256 dip values are stored in an array called DIP and should have the desired mean, standard deviation, and spatial covariance. The number 256 is used because it is a power of 2 (appropriate for the FFT computer algorithm) and will generally provide more than enough fracture values to fill the face of a 15-to-25-m-high mine bench with plane shear fractures. Also, this simulation method is not a Monte Carlo-type simulation, because Monte Carlo simulated values are random and independent of each other.

2.  FFT is used to simulate 256 spatially dependent, exponentially distributed values of fracture set **spacing** for the identified plane shear fracture set. These 256 spacing values are stored in an array called SPA and should have the desired mean, standard deviation, and spatial covariance.

3.  FFT is used to simulate 256 spatially dependent, exponentially distributed values of fracture set **waviness** for the identified plane shear fracture set. These 256 waviness values are stored in an array called **WAV** and should have the desired mean, standard deviation, and spatial covariance.

4.  A uniform U[0, 1] number ($u_o$) is generated and then multiplied by mean spacing of the fracture set to establish a random starting point near the toe of the bench face where the first plane shear fracture of the simulated plane shear set will be positioned. The distance measured from the bench toe up the bench face to this position is given by—

$$\text{Starting distance (meters)} = u_o\,(\text{SMU}) \quad \text{(F-8)}$$
$$= \text{FID}(1,1)$$

where $u_o$   =   uniform U[0,1] random number,

SMU   =   mean spacing of plane shear fracture set (meters),

and FID(1,1) =   array element equal to distance to first simulated fracture .

5.  Additional first-array elements are assigned as follows:

    FID(2,1)  = first simulated fracture dip value = DIP(1),

    FID(3,1)  = first simulated fracture waviness value = WAV(1),

    and  FID(4,1)= required length for first fracture to extend from bench face to breakout point on top of bench

    = {(bench height) - FID(1,1)[sin(A)]}/sin[DIP(1)],

    where  A  = bench angle.

6.  Each successive fracture array element k is defined using the previous $j = k - 1$ element, as plane shear fractures in the bench are stacked until they intersect the bench face all the way up to the bench crest.

    $$FID(1,k) = FID(1,j) + \quad (F\text{-}9)$$
    $$+ SPA(j)/\sin(A - DMU),$$

    where A  =  bench angle,

    DMU  =  mean dip of fracture set,

    FID(2,k) =  DIP(k),

    FID(3,k) =  WAV(k),

    and  FID(4,k) =  {(bench height) - FID(1,k)[sin(A)]}/ sin[FID(2,k)].

7.  The probability that each k-th fracture will be longer than FID(4,k) is calculated using an assumed exponential distribution for fracture set length (that is, the fracture is of sufficient length to form a planar, continuous slope-failure surface).

    $$P[L > FID(4,k)] = 1 - \quad (F\text{-}10)$$
    $$- \{1 - \exp[-FID(4,k)/ LMU]\}$$

    where  LMU = mean length of fracture set.

8.  The probability of sliding (that is, that the safety factor is less than 1.0) is calculated for the plane shear failure block defined by each k-th fracture using the point estimation method that relies on fracture waviness, fracture dip, fracture set shear strength, and unit weight of the rock mass. The probability that the plane shear block defined by the k-th fracture will not slide is then given by—

$$P_{nonslide}[\text{k-th plane shear block}] = 1 - P_{slide}[\text{k-th plane shear block}]. \quad (F\text{-}11)$$

9.  For the k-th plane shear block to be stable, either the k-th fracture is not long enough to allow failure **or** it is long enough and the block does not slide.

$$P_{stab.}[\text{k-th plane shear block}] = \{1 - P[L > FID(4,k)]\} + \quad (F\text{-}12)$$
$$+ \{P[L > FID(4,k)]\} \{P_{nonslide}[\text{k-th plane shear block}]\}.$$

10. For any given back-break cell to be stable on the top of the simulated bench, all plane shear fractures that break out in that cell must be stable. Thus, cell stability is represented by the joint probability of plane shear stability, or the product (multiplication) of the corresponding $P_{stab.}$ values for that given cell.

11. Steps 1 through 10 are repeated for *n* bench simulations. Cell stability values are accumulated and then averaged (see Eq. F-1). The probability of retaining a specified bench width by combining the appropriate cell stability values is calculated.

# APPENDIX G: VOLUME OF FAILED MATERIAL

Estimated volumes of rockfall debris generated by bench failure can be related directly to the probability of retaining given catch-bench widths. If the probability associated with a specified back-break cell is calculated as $P_i$, then the average failure volume associated with $P_i$ can be estimated. First, calculate $h_f$, the vertical height of an average failure.

$$h_f = C_i (\sin D \cdot \sin B)/\sin(B-D), \quad \text{(G-1)}$$

where $C_i$ = back-break distance to center of cell with probability $P_i$,

$\quad B$ = bench face angle,

and $\quad D$ = average dip of plane shears or average plunge of wedges in the simulation.

Then, calculate the unit width area (that is, the area associated with a 1-m increment along a bench run).

$$A_i = 0.5h[C_i + (h/\tan B)] \quad \text{(G-2)}$$

The associated intact volume of rock prior to the failure is then $V_i = A_i \times 1 \text{ m}^3$ of rock per meter of bench run. A bulking factor (usually 1.20 to 1.35) then is multiplied by this volume to estimate the volume of loose rock and debris lost from the bench crest and which must be contained on the catch bench below. If this volume exceeds the expected storage volume on the lower bench, then the debris can be expected to cascade farther down the overall slope.

# APPENDIX H: INPUT PARAMETERS

Table H-1.—Input Parameters

| Parameter | Bplane | Bstepp | Bwedge |
|---|---|---|---|
| **Bench** | | | |
| Bench height and width (m) | | | |
| The physical dimensions of a bench in a vertical section through the rock slope. | X | X | X |
| Number of bench cells | | | |
| Back-break cells are defined to discretize bench width to examine failure potential. A cell is considered to have failed when it contains any portion of a failing block. Typically, the cells are 1 m wide, but they can be adjusted to provide greater or smaller resolution. For instance, if maintaining a 2.5-m-wide bench is deemed to be critical, a cell width of 0.5 m could be used, ensuring that results would be reported for the 2.5-m width. If a width of 1 m were used, results would be reported for full meter increments only. | Figure H-1 | Figure H-2 | Figure H-3 |
| Height of ground water above bench toe (m) | | | |
| The effect of water saturation can be introduced through calculations of pore pressure. Water level is assumed to be at a constant height above the toe throughout the slope and is used to compute effective stresses in the joint stability criterion. | X | X | X |
| Slope angle (degrees) | | | |
| Design dip of bench face | X | X | X |
| Number of lines, distance 1, distance 2, .. (m) | | | |
| These lines are defined along the face and serve, in combination with backbreak cells, to discretize the bench for failure analysis (figure 17). The first parameter indicates the number of lines. The subsequent values are the distances from slope crest to each line. The program seeks to identify failures within these cells that might occur within a section of slope as long as it is high. Cells containing failing wedges are considered to have failed. Thus, results should be interpreted as the probability that a segment of slope as long as it is high will have a minimum width everywhere along this segment. Results can be sensitive to the location of these lines. Such sensitivity can be evaluated by repeating the analysis with various line locations. | | | X |
| **Fractures** | | | |
| Fracture length mean (m) | | | |
| *Bplane and Bstepp* assume that fractures are of sufficient length parallel to the bench so that the stability of blocks is not affected by terminations of the fractures along bench strike. | X | X | |
| *Bwedge* considers that fracture length is three-dimensional and invariant with direction. | | | X |
| *Bplane*:  Fracture lengths are assumed to vary within an exponential probability density function defined by its mean. This function is defined entirely by one parameter, since standard deviation and mean of this function are, by definition, equal for the exponential probability density function. | X | | |
| *Bstepp*:  The user enters the minimum and maximum lengths for both master- and cross-joint fracture sets. These values are used to define a beta probability distribution of fracture lengths. This distribution is bounded by the minimum and maximum values with lengths clustered in the lower one-third of the range (a skewed-right probability density function with beta parameters $P = 1$ and $Q = 4$). | | X | |
| Fracture spacing mean (m) | | | |
| Fracture spacing is the distance between fractures measured perpendicular to the fracture planes. If fracture planes are wavy or otherwise vary in orientation, the mean is the spacing between fractures of average orientation. | X | X | X |

(Continued)

Table H-1 (Continued).—Input Parameters

| Parameter | Bplane | Bstepp | Bwedge |
|---|---|---|---|
| Fracture spacing nugget (m$^2$) | | | |
| Fracture spacing nugget (that is, the y-intercept on the variogram plot) describes measurement error and/or short-scale variability of fracture spacings within a set. The exponential probability density function and a spherical variogram model are used to describe variability of fracture spacing. Thus, sill variance is defined as mean spacing squared, and the nugget must not exceed this value. If sill variance and nugget are equal, spatial dependence is absent, and fracture spacing varies randomly across space for this fracture set. | X | X | X |
| Fracture spacing range (number of fractures) | | | |
| Fracture spacing range is expressed as a number of fractures and generally describes the distance (in terms of fracture count) at which spacing between fracture pairs loses spatial dependence. The range of a *spherical variogram model* is defined as the distance (in terms of a fracture count) at which the variogram model reaches the sill. The sill for fracture spacing is equal to the mean squared (that is, the sample variance assuming an exponential probability density function). | X | X | X |
| Fracture waviness (degrees) | | | |
| Fracture waviness is used to account for large-scale roughness that is neglected in small-scale tests of joint strength. It is defined as the difference between average and minimum dip. Fracture waviness is discussed in more detail in the section on "Waviness." Fracture waviness is described by a skewed right beta distribution (P = 1, Q = 4). | X | X | X |
| Fracture dip | | | |
| Fracture dip mean (degrees) | | | |
| Fracture dip is modeled by a normal probability density function. If multiple fracture sets are involved (Bstepp, Bwedge), each should be entered separately. The probability of maintaining a given bench width will be the joint probability of maintaining the width for each fracture set (or pair of fracture sets in Bwedge). | X | X | X |
| Fracture dip nugget (degrees squared) | | | |
| The fracture dip nugget (that is, the y-intercept on the variogram plot) describes measurement error and short-scale variability of fracture dip within a set. This value should not exceed the sill value. If the nugget is equal to sill variance, there is no spatial dependence, and dip varies randomly. | X | X | X |
| Fracture dip range (number of fractures) | | | |
| The range of a spherical variogram model is defined as the distance (in terms of a fracture count) at which the variance equals the sill value. | X | X | X |
| Fracture dip standard deviation (degrees) | | | |
| The standard deviation of a normal probability density function approximating the population of fracture dips. The square of the standard deviation is the sill for the spherical variogram model. | X | X | X |
| Fracture dip direction mean (degrees) | | | |
| Mean dip direction of the fracture set being modeled. | | | X |
| Fracture dip direction standard deviation (degrees) | | | |
| The standard deviation of fracture dip directions. The square of the standard deviation is the sill, or variance between pairs of fractures at great distance, in the spherical variogram model. | | | X |
| Fracture dip direction nugget (degrees squared) | | | |
| The fracture dip direction nugget (that is, the y-intercept on the variogram plot) describes measurement error and/or short-scale variability of fracture dip direction within a set. This value should always be less than the sill. | | | X |
| Fracture dip direction range (number of fractures) | | | |
| The fracture dip direction range is expressed as a number of fractures and generally describes the distance (in terms of number for fractures) at which fracture dip direction loses spatial dependence. The range of a spherical variogram model is defined as the distance (in terms of a fracture count) at which the variogram model reaches the sill. | | | X |

(Continued)

Table H-1 (Continued).—Input Parameters

| Parameter | Bplane | Bstepp | Bwedge |
|---|---|---|---|
| Rock mass | | | |
| Rock density mean (t/m$^3$) | | | |
| An estimate of the bulk density of the rock is needed to compute the weight of blocks and wedges having the potential to slide. Density is modeled as a constant. Typical values range from 2.50 to 2.70 t/m$^3$. | X | X | X |
| Maximum intact rock gap (m) | | | |
| This parameter does not affect the geometry or the properties of the step-paths generated. Rather, it helps the program differentiate between potentially sliding step-paths and those that are stable (that is, step-paths with intact rock bridges that are too large to fail). The program assumes that any step-path containing a rock bridge longer than the maximum intact rock gap will be stable, limiting the range of paths that must be analyzed further. Failures along surfaces that involve rupture of large amounts of intact rock (usually weak rock or soil) are best considered using other methods. Typical values for this maximum gap range from 0.02 to 0.15 m. Input must be in meters. | | X | |
| Rock tensile strength mean (t/m$^2$) | | | |
| Mean tensile strength of intact rock, particularly rock that will likely form bridges separating master and/or cross joints. | | X | |
| Rock tensile strength standard deviation (t/m$^2$) | | | |
| Standard deviation of rock tensile strength, particularly rock that will likely form bridges separating master and/or cross joints. Variation of tensile strength is modeled by a normal probability density function modified by setting minimum and maximum bounds at ±4 standard deviations. In addition, minimum tensile strength is not allowed to be negative. Values generated beyond these bounds are set equal to the exceeded bound. | | X | |
| Shear strength parameters (a, b, and c) | | | |
| These parameters define a general power-curve model that relates shear strength to effective normal stress. | X | X | X |

$$\tau = a\sigma^b + c,$$

where $\tau$ = shear strength (t/m$^2$),

$\sigma$ = effective normal stress (t/m$^2$),

and a, b, c = model parameters.

| | Bplane | Bstepp | Bwedge |
|---|---|---|---|
| This model reverts to the familiar Mohr-Coulomb linear model of friction if b is set equal to 1. In this case, a is the tangent of the friction angle, and c is cohesion. These parameters are discussed in more detail in section 5.2.1. Typical ranges for these values are 0.3 to 2.0 t/m$^2$ for a; 0.5 to 1.0 for b; and 0.0 to 6.0 for c. | | | |
| *Bstepp*: Shear strength is defined only for the master-joint fracture set. Sliding will not occur on cross-joint fractures. Cross joints open and are assumed to have no strength in tension. | | X | |
| Shear strength standard deviation (t/m$^3$) | | | |
| Typical values of the shear strength standard deviation range from 0.2 to 0.6 t/m$^2$. | X | X | |
| Shear strength coefficient of variation | | | |
| The coefficient of variation is defined as the standard deviation divided by the mean (in this case, shear strength standard deviation divided by mean shear strength). A coefficient of zero implies no variation from the mean, while higher values show increased variation of strengths around the mean. Typical values range from 0.2 to 0.4. | | | X |

(Continued)

61

Table H-1 (Continued).—Input Parameters

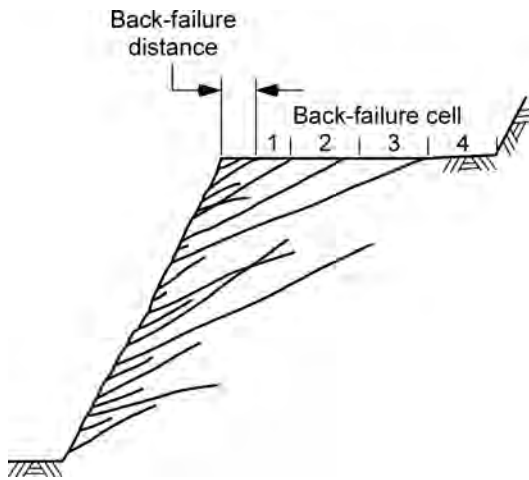| Parameter | Bplane | Bstepp | Bwedge |
|---|---|---|---|
| Computer entries | | | |
| Random seed | | | |
| A five-digit integer is input to Aseed@ the random number generator used to develop input to each simulation. The generated numbers are random in the sense that the likelihood of a given value being generated is independent of the magnitude of that value. However, the sequence of generated numbers follows predictably from any given seed value. The influence of the seed value on results will be greatest for a single simulation and will decline as the number of simulations is increased. The influence of the seed value on an analysis can be checked by repeating the run with a different seed value. If results vary significantly with seed value, then the number of simulations should be increased. | X | X | X |
| Number of simulations | | | |
| Each simulation, or "sim," involves randomly generating a specific set of fractures and fracture properties (Bplane and Bwedge) or step-paths and related properties (Btepp) consistent with the statistical distributions and then testing whether blocks defined by these fractures or step-paths have the potential to slide. Each simulation produces a plausible result, or one plausible realization. Many simulations are required to estimate the true likelihood that various bench widths will be maintained. Adequacy can be checked by seeing if results change significantly for a small increase or decrease in the number of sims or for a change in random seed.<br>   *Bplane* is capable of running up to 200 simulations, but 100 should be adequate for most situations.<br>   *Bstepp*: Bstepp is capable of running up to 100 simulations. Fifty sims should be considered minimal for most situations.<br>   *Bwedge*: Sixty sims will be sufficient in many cases, but the maximum of 200 sims may be desirable in others. The sensitivity of results to the number of sims can be checked by making runs with slight variations in number of sims. | X | X | X |
| Output file | | | |
| Name of the output file, including file extension. | X | X | X |
| Compute button | | | |
| Clicking on the compute button starts a run, which consists of checking input against a set of limits; saving the input to a file named Bplane.tmp, Bstepp.tmp, or Bwedge.tmp, as appropriate; computing the probabilities of retaining various bench widths; and then writing results to the specified output file. A "Computing–Please Stand By" message is displayed during calculations. This window will persist after calculations are complete. The input window will reappear when a run has been completed, displaying sample results. | X | X | X |

Figure H-1. Back-break cells plotted on a typical bench for a Bplane analysis. Each cell will be considered to have failed if a plane failure intersects the bench anywhere within the cell.
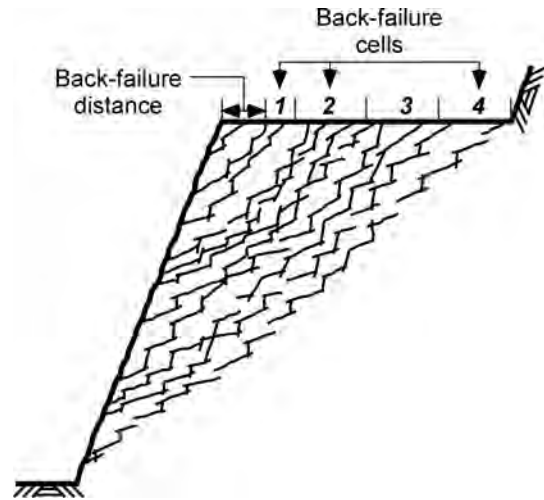


Figure H-2. Back-break cells plotted on a typical bench for a Bstepp analysis. Each cell will be considered to have failed if a step-path failure intersects the bench anywhere within the cell.
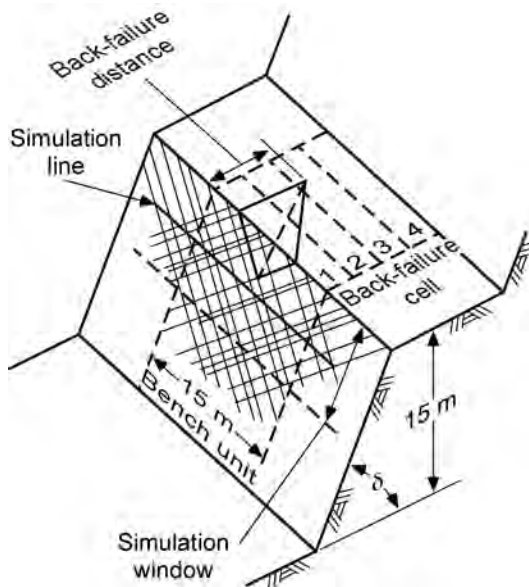


Figure H-3. Discretization of bench width with cells and slope face with lines for a Bwedge analysis.

**Bplane** *parameter values.* Input parameters are screened for reasonable ranges. Error messages are generated for values outside the following ranges:

| | |
|---|---|
| Bench height | 1 – 80 m |
| Bench width | 1 – 80 m |
| Bench cell increment | Less than or equal to 20 |
| Ground water height | Less than bench height |
| Density | 1.9 – 2.9 t/m$^3$ |
| Slope angle | 20° – 89° |
| Fracture length mean | 0.1 – 50 m |
| Fracture dip mean | Positive and less than the slope angle |
| Fracture dip standard deviation | Positive and less than 10° |
| Fracture dip nugget | Positive and less than dip standard deviation squared |
| Fracture dip range | 1 to 30 fractures |
| Fracture spacing mean | 0.05 – 5 m |
| Fracture spacing nugget | Positive and less than mean spacing squared |
| Fracture spacing range | 1 to 30 fractures |
| Fracture waviness | 0° – 12° |
| Fracture maximum waviness | Greater than minimum waviness |
| Shear strength a coefficient | Positive and less than 3 |
| Shear strength b coefficient | 0.3 to 1 |
| Shear strength c coefficient | 0 – 2 t/m$^2$ |
| Shear strength standard deviation | 0.2 – 0.6 t/m$^2$ |
| Number of simulations | Less than or equal to 200 |

***Bstepp*** *parameter values*. Input parameters are screened for reasonable ranges. Limits apply to both master and cross joints unless otherwise noted. Error messages are generated for values outside the following ranges:

| | |
|---|---|
| Bench height | 1 – 80 m |
| Bench width | 1 – 80 m |
| Bench cell increment | Less than or equal to 20 |
| Ground water height | Less than bench height |
| Density | 1.9 – 2.9 $t/m^3$ |
| Intact rock tensile strength | 100 – 2000 $t/m^2$ |
| Tensile strength standard deviation | Less than 100 $t/m^2$ |
| Slope angle | 20° – 89° |
| Maximum fracture length | Less than or equal to 20 m |
| Minimum fracture length | Greater than or equal to 0.2 m |
| Master joint mean dip | Less than the slope angle |
| Cross-joint mean dip | 60 – 110° (dip > 90° for overturned sets) |
| Fracture dip standard deviation | Less than 10° |
| Fracture dip nugget | Less than dip standard deviation squared |
| Fracture dip range | 1 to 30 fractures |
| Fracture spacing mean | 0.05 – 5 m |
| Fracture spacing nugget | Less than mean spacing squared |
| Fracture spacing range | 1 to 30 fractures |
| Fracture waviness | 0° – 12° |
| Fracture maximum waviness | Greater than minimum waviness |
| Shear strength a coefficient | 0.1 – 3 |
| Shear strength b coefficient | 0.3 – 1 |
| Shear strength c coefficient | 0 – 10 $t/m^2$ |
| Shear strength standard deviation | 0.2 – 0.6 $t/m^2$ |
| Number of simulations | 50 to 100 |

***Bwedge*** *parameter values.* Input parameters are screened for reasonable ranges. Error messages are generated for values outside the following ranges:

| | |
|---|---|
| Bench height | 1 – 80 m |
| Bench width | 1 – 80 m |
| Bench cell increment | Less than or equal to 20 |
| Ground water height | Less than bench height |
| Density | 1.9 – 2.9 t/m³ |
| Slope and fracture dips | 20° – 89° |
| Slope face dip direction | 0 – 360° |
| Fracture dip directions | 0 – 360° |
| Fracture dip direction standard deviation | 0 – 15° |
| Fracture dip direction nugget | Positive and less than dip direction range squared |
| Fracture dip direction range | 1 to 30 fractures |
| Fracture dip standard deviation | 0 – 8° |
| Fracture dip nugget | Less than dip standard deviation squared |
| Fracture dip range | 1 to 30 fractures |
| Fracture length mean | 0.1 – 50 m |
| Fracture spacing mean | 0.05 – 5 m |
| Spacing nugget | Less than mean spacing squared |
| Spacing range | 1 to 30 fractures |
| Shear strength a coefficient | 0.1 – 3 |
| Shear strength b coefficient | 0.3 – 1 |
| Shear strength c coefficient | 0 – 10 t/m² |
| Shear strength coefficient variance | 0.2 – 0.6 |
| Fracture waviness | 0° – 12° |
| Fracture maximum waviness | Greater than minimum waviness |
| Simulation line distance | Less than or equal to bench height |
| Number of simulation lines | 1 – 4 |
| Simulation line spacing | Not less than 0.5 m |
| Number of simulations | Less than or equal to 200 |

# NIOSH

## Delivering on the Nation's promise:
*Safety and health at work for all people through research and prevention*

To receive documents or more information about occupational safety and health topics, contact NIOSH at

Phone: 1-800-35-NIOSH (1-800-356-4674)
Fax: 513-533-8573
E-mail: pubstaff@cdc.gov

or visit the NIOSH Web site at www.cdc.gov/niosh

## SAFER • HEALTHIER • PEOPLE™